

A comprehensive calibration framework for the Northwest River Forecast Center

Geoffrey Walters^{a,1}, Cameron Bracken^{b,2}, Brad Gillies^{a,3}, Leah Pope^{a,4}, Sonali Chokshi^{a,5}, Victor Stegemiller^{a,6}, Julie Bracken^{c,7}, Stephen King^{b,8}, Taylor Dixon^{d,9}, Joe Intermill^{b,10}

^a Northwest River Forecast Center

^b Pacific Northwest National Laboratory

^c Portland State University

^d Center for Western Weather and Water Extremes

This is a non-peer reviewed preprint submitted to EarthArXiv. The manuscript was submitted for publication in the *Journal of the American Water resources Association*. Please contact the lead author with any comments or questions.

¹geoffrey.walters@noaa.gov

²cameron.bracken@pnnl.gov

³bradley.gillies@noaa.gov

⁴leah.pope@noaa.gov

⁵sonali.chokshi@noaa.gov

⁶victor.stegemiller@noaa.gov

⁷jbracken@pdx.edu

⁸stephen.king@noaa.gov

⁹t3dixon@ucsd.edu

¹⁰jsintermill@msn.com

RESEARCH ARTICLE

A comprehensive calibration framework for the Northwest River Forecast Center

Geoffrey Walters¹ | Cameron Bracken² | Brad Gillies¹ | Leah Pope³ | Henry Pai¹ |
Sonali Chokshi¹ | Victor Stegemiller¹ | Stephen King¹ | Taylor Dixon⁴ | Julie Bracken⁵ |
Joe Intermill¹

¹Northwest River Forecast Center, National Weather Service, Oregon, USA

²Pacific Northwest National Laboratory, Washington, USA

³Portland Weather Forecast Office, National Weather Service, Oregon, USA

⁴Center for Western Weather and Water Extremes, California, USA

⁵Portland State University, Oregon, USA

Correspondence

Corresponding authors:

Geoffrey Walters,

Email: geoffrey.walters@noaa.gov

Cameron Bracken,

Email: cameron.bracken@pnln.gov

Abstract

We present a comprehensive framework developed by the Northwest River Forecast Center for calibrating hydrologically diverse basins. The framework includes models for snow, soil moisture, routing, channel loss, and consumptive use. Data inputs include a wide range of open-access datasets for meteorology, land use, topography, and land cover. The framework uses conceptual hydrologic models to handle basins with various hydrologic regimes including rain-driven and snowmelt-dominated basins. We also develop a flexible automatic calibration system that can handle numerous unobservable model parameters in a computationally efficient manner. A single-basin automatic calibration run can typically be completed on a modern laptop in under 10 minutes. We found that model performance metrics for this new approach match the quality of the NWRFC's previous labor-intensive manual calibrations. The model performance also rivals that of a state-of-the-art deep learning model at a fraction of the computational cost. This framework presents a new standard for the quality of calibrations possible with lumped conceptual hydrologic models, combining careful data curation, an objective calibration framework, and expert local knowledge. In addition, we have made software packages available for the entire suite of National Weather Service River Forecast System models, including SAC-SMA, SNOW-17, and Lag-K. These modern interfaces are intended to increase accessibility and facilitate future research.

KEY WORDS

hydrology, calibration, automatic calibration, operational forecasting, open source software, conceptual modeling

1 | INTRODUCTION

The Northwest River Forecast Center (NWRFC) is one of thirteen River Forecast Centers (RFC) that are part of the United States (US) National Weather Service (NWS), which is in turn part of the National Oceanic and Atmospheric Administration (NOAA). The NWRFC's operational mission includes (1) modeling rivers across the Pacific Northwest in the Columbia River Basin and Coastal Basins in Washington and Oregon, (2) providing seasonal water volume forecasts and guidance for the region, and (3) supporting decision-making while collaborating with NWS core partners. These partners include federal, state, and local government agencies and private companies that oversee water management, environmental stewardship, power generation, and emergency response. The Pacific Northwest region is composed of a wide range of hydrologic conditions including rain-dominated, snowmelt-dominated, glaciated, tidally influenced, and arid basins. Some watersheds exist in Canada and eventually flow into the US. Forecasts developed by the NWRFC are used across the region to provide timely information about flooding, water supply, drought, recreation, navigation, and environmental flows.

The NWRFC utilizes a suite of hydrologic models developed by the NWS representing snow, soil moisture, routing, channel loss, and consumptive use processes to develop river forecasts for numerous points across the region. The NWS River Forecasting

System (NWSRFS) was initially developed in the late 1970s but continues to be utilized today as part of the NWS Community Hydrologic Prediction System (CHPS) (Anderson 2002 and Schaake et al. 2006). Hydrologic forecasts produced by the NWS RFCs remain the official river forecasts of the NWS, providing stage and streamflow forecasts at approximately 3600 discrete locations within watersheds that flow into and through the US and its territories. The NWS Office of Water Prediction (OWP) also provides unofficial river forecasting guidance using the National Water Model (NWM) (Cosgrove et al. 2024), which is an independent modeling system from those used operationally by the RFCs.

Periodically the NWRFC recalibrates its suite of models as new data and methods become available. In previous iterations, calibration was a mostly manual and labor-intensive process. In 2018, the NWRFC began an effort to modernize its calibration approach by using a new forcing dataset, new zone delineations, better representing hydrologic fluxes, transparently validating models, expanding performance metrics, and applying modern computational capabilities via an automatic calibration system.

To translate precipitation into streamflow, RFCs rely on three models: SNOW-17 for snow accumulation and ablation, the Sacramento Soil Moisture Accounting Model (SAC-SMA) for hillslope routing, and UNIT-HG for inner basin routing. While the NWRFC employs all three models in conjunction, other RFCs operating in regions with minimal snowmelt will omit SNOW-17. Previous studies have successfully used auto-calibration with some or all of these models. Newman et al. (2015) auto-calibrated these models for 671 headwater basins across the contiguous US spanning a range of hydrologic conditions. They calibrated 11 SAC-SMA parameters, 6 SNOW-17 parameters, and 2 parameters for UNIT-HG with a Root Mean Square Error (RMSE) objective function. RMSE-like objective functions more heavily weight high flows due to the square term, which can be a benefit for flood applications but can produce biased or poor quality simulations during low flow periods. Gupta et al. (1998) used multiobjective optimization to calibrate 13 SAC-SMA parameters. While multiobjective optimization can provide valuable information about tradeoffs and model limitations, it can be difficult to use in an operational setting where a single calibrated model is needed. Hogue et al. (2000) developed a multistep auto-calibration scheme which mimics the best aspects of a manual calibration process but cuts down on the overall time spent calibrating. They calibrated 15 parameters overall in a 3-step process. Chouaib et al. (2021) calibrated 13 SAC-SMA parameters in the Eastern US using the Shuffle Complex algorithm (SCE-UA) which has been shown to work well with smaller parameter sets but struggles with a larger number of parameters.

Recent advances in deep learning, specifically long short-term memory (LSTM) models, have been applied to hydrologic modeling with impressive results (Feng et al. 2022 and Konapala et al. 2020 and Kratzert et al. 2019 and Nearing et al. 2021 and Shen 2018). While these approaches perform well for unimpaired basins, capturing the effects of reservoir regulation and water withdrawals is difficult due to lack of data and nonstationary human water management and use practices. Operational river forecasting must include accurate reservoir operations, water withdrawals, and routing from upstream reaches. In the US, this involves active coordination between multiple federal, state, and local water management agencies, as well as private utilities who oversee releases from their respective reservoirs.

In this paper, we present a comprehensive approach for hydrologic model calibration for use at the NWRFC that is tailored for an operational setting. Our goals were to develop a flexible, reproducible, high-performing auto-calibration methodology that can accommodate most NWRFC basins. The diversity of models calibrated include those with multiple zones, routed upstream flow, channel losses, consumptive use, and up to 90 parameters. Section 2 discusses the existing modeling system at the NWRFC, Section 3 describes the data used for calibration, Section 4 discusses the auto-calibration system developed by the NWRFC for model parameterization, Section 5 describes the software packages which call the NWSRFS models that have been publicly released, Sections 6 and 7 provide calibration results, and Section 8 provides discussion and conclusions.

2 | EXISTING MODELING SYSTEM

The NWRFC uses a suite of models available to all RFCs to forecast stage and streamflow at a location. The location of the forecast point normally coincides with longstanding streamflow observation gages like those maintained by the United States Geological Survey (USGS). Typically a streamflow gauge needs an observed record of at least ten years to be a suitable candidate as the basis for model calibration in order to include the forecast point operationally. Figure 1 illustrates the NWRFC domain, including forecast points (black dots) and prominent river reaches (blue lines). To provide geographic context, the Columbia and Snake River mainstems, the two largest river systems in the NWRFC domain, are emphasized with increased line weights. Each forecast point represents a distinct NWSRFS model segment, interconnected via hydrologic routing and requiring rigorous calibration before operational deployment. The grey shaded areas represent unimpaired basins from the Catchment Attributes and Meteorology for Large-sample Studies (CAMELS) dataset (Newman et al. 2015 2022), further detailed in Section 6. Finally, the colored watersheds highlight the three specific basins selected for the case studies presented in Section 7.

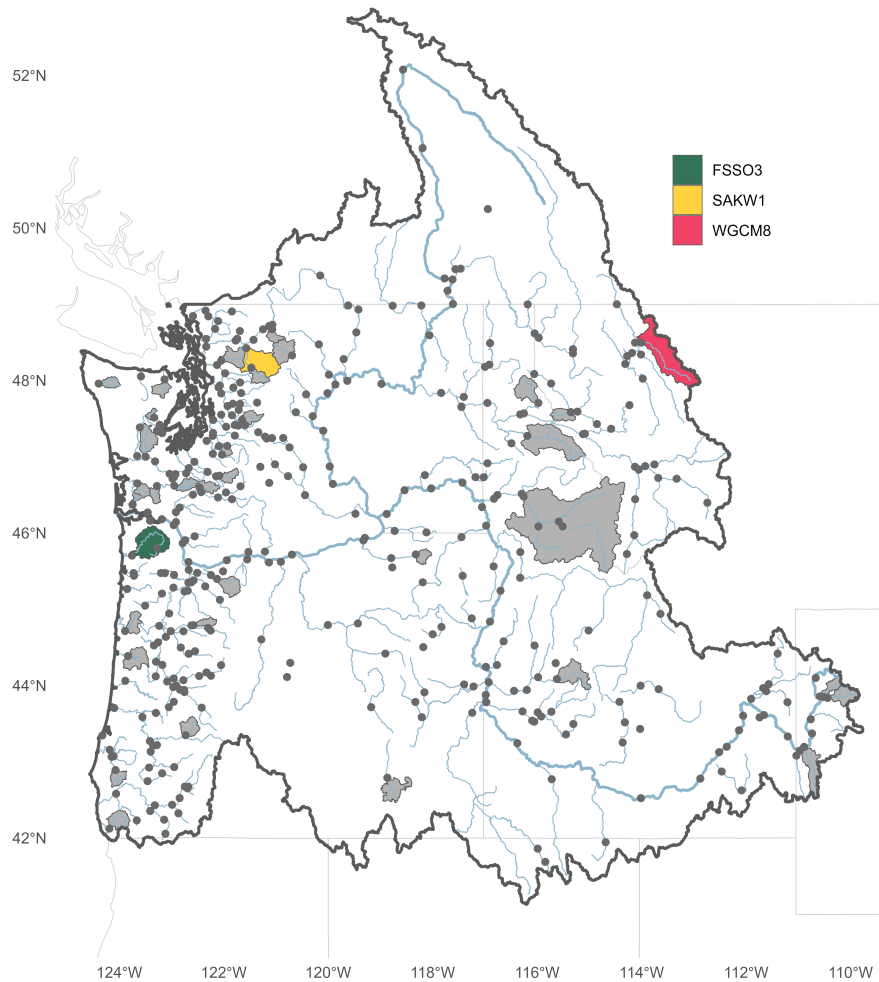


FIGURE 1 Map of the NWRFC domain (thick black outline), forecast points (black dots), and primary river reaches (blue lines). The mainstems of the Columbia and Snake Rivers are highlighted with increased line weight. CAMELS basins are shaded grey, while the three case-study basins are highlighted in color.

70 The NWRFC model suite is composed of three core models to translate precipitation to streamflow (SNOW-17, SAC-SMA,
 71 and UNIT-HG), the Lag-K hydrologic routing model, and three supplemental models used for specific circumstances. The
 72 supplemental models are Channel Loss (CHANLOSS) for computing losses and gains along river reaches, the Consumptive
 73 Use Operation (CONS_USE) for irrigation water withdrawals, and Streamflow Synthesis and Reservoir Regulation System
 74 (SSARRESV). For any given basin, the supplemental models can be deployed in any combination, or omitted entirely, to modify
 75 the simulations produced by SNOW-17, SAC-SMA, UNIT-HG, and/or by Lag-K.

76 The general procedure for linking these models in an operational setting is as follows: SNOW-17 requires meteorological
 77 inputs of precipitation accumulation, air temperature, and percent precipitation as snowfall (PTPS) to produce an estimate of
 78 rain plus melt runoff (RAIM). SAC-SMA uses RAIM and evapotranspiration demand (ETD) as modeling input and simulates
 79 water moving through both the shallow soil column and overland flow to produce total overland and channel flow (i.e. runoff).
 80 The runoff is routed to the basin outlet with the UNIT-HG model. The Lag-K model accounts for the lag and attenuation of
 81 streamflow routed from upstream forecast points. If the watershed characteristics dictate it, the streamflow simulation can be
 82 further modified by any of the three supplemental models to accurately capture gains, losses, or storage. Figure 2 shows the
 83 connectivity of these models.

84 A single instance of the set of models can be used to represent the entire lumped watershed, or alternatively, multiple model
 85 sets can be used to represent discrete portions of the basin, often referred to by the RFCs as zones. Each zone (traditionally
 86 delineated based on elevation) has its own unique parameter set corresponding to SNOW-17, SAC-SMA, and UNIT-HG. The

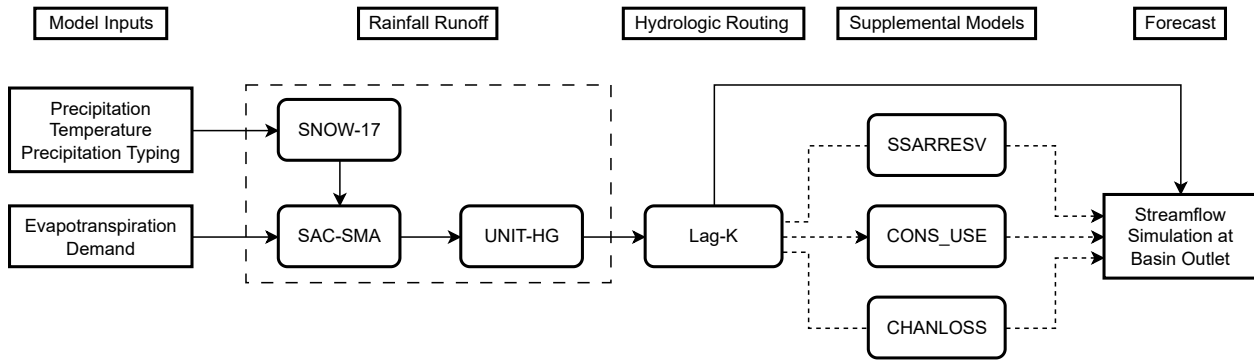


FIGURE 2 The operational models used by the NWRFC for forecasting. See Section 2 for complete details on each model.

87 simulated streamflows from each zone are combined to produce the total basin contributing flow at the outlet before Lag-K and
 88 the supplemental models are applied as needed. The following sections provide an overview of the models used by the NWRFC
 89 for operational forecasting; for complete technical specifications, please refer to the relevant manuals.

90 2.1 | SNOW-17 - Snow Accumulation and Ablation

91 The SNOW-17 model is a lumped temperature-indexed snow accumulation and ablation model (National Weather Service
 92 2006). The time series inputs to SNOW-17 are precipitation accumulation, air temperature, and PTPS. The physical processes of
 93 accumulation and ablation of snow cover are captured by the model but in a simplified form. The model uses precipitation and
 94 PTPS to inform the accumulation of snowmelt. The model captures air temperature sensitivity and its impact on the melt rate
 95 through the use of a seasonally varying melt factor (Figure 3, left). The energy and mass balance are captured in an accounting
 96 component within the model that tracks the snowpack heat deficit, liquid water ratio, and snow-covered area. The heat deficit
 97 needs to rise to 0°C and the melted water stored in the snowpack has to rise above the capacity of the pore space to begin the
 98 onset of melt. The model's state of the snow cover controls the amount of melt, where more water is made available as melt
 99 when there is more simulated snow cover (National Weather Service 2006). The primary output of the SNOW-17 model is a
 100 time series of simulated RAIM for the modeled basin or zone which is used as an input to SAC-SMA. SNOW-17 also outputs
 101 several state variables such as snow water equivalent (SWE) depth and areal extent of snow cover (AESC) which are useful
 102 operationally to validate and tweak model performance.

103 2.1.1 | Glacial Zones in SNOW-17

104 Eleven basins within the NWRFC domain contain permanently glaciated areas; these are delineated into distinct zones to
 105 accommodate their specialized model configurations (Anderson 2002). The SNOW-17 model for glacial zones must account
 106 for effectively unlimited available melt. The approach for modeling glacial zones with SNOW-17 differs in three key ways.
 107 First, the initial snow water equivalent depth is set very high so that it never melts off completely. Second, the liquid water ratio
 108 accounting is turned off. Finally, the snow is always assumed to cover the entire area. Other components of the SNOW-17 model,
 109 such as seasonally varying melt factor and the heat deficit, are modeled similarly to non-glaciated zones.

110 2.2 | SAC-SMA - Hillslope Runoff

111 SAC-SMA is a conceptual soil moisture and hillslope runoff model (Burnash et al. 1973 and National Weather Service 2002a).
 112 SAC-SMA inputs are RAIM from the SNOW-17 model and a time series of ETD. The model contains several interconnected
 113 parameterized buckets which fill and drain according to the model parameters. These buckets simulate discrete aspects of the
 114 rainfall-runoff process such as impervious runoff, surface runoff, interflow, and baseflow (Figure 3, right). SAC-SMA also
 115 accounts for losses from evapotranspiration, riparian vegetation, and deep ground water recharge. The model parameters are not

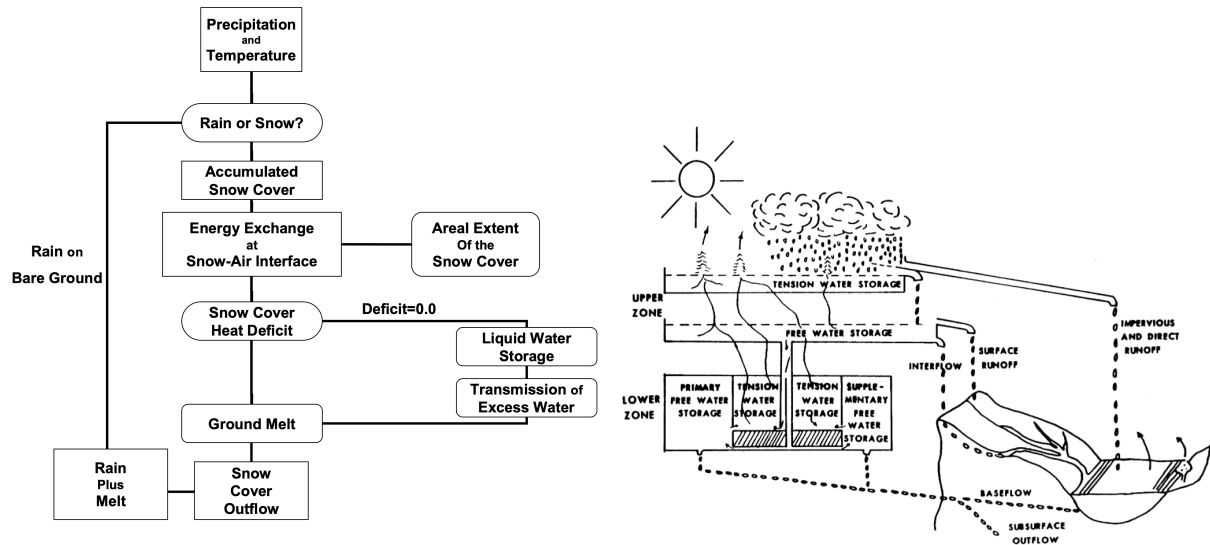


FIGURE 3 SNOW-17 diagram (left) from National Weather Service (2006) and SAC-SMA diagram (right) from National Weather Service (2002a).

116 calibrated by sampling the soil profile via field studies, but rather through inference using observations of rainfall and streamflow.
 117 A more detailed overview of the SAC-SMA model is provided in the manual (National Weather Service 2002a).

118 2.2.1 | Glacial Zones in SAC-SMA

119 For glacial zones, only certain components of SAC-SMA are used, primarily those that control the attenuation of water through
 120 the soil column due to the frozen ground conditions. The following components are disabled: tension water storage, impervious
 121 runoff, evapotranspiration, and losses from riparian vegetation (Anderson 2002).

122 2.3 | UNIT-HG - Inner Basin Routing

123 The primary output of SAC-SMA is a time series of combined overland and channel flow which represents the available water in
 124 a basin that needs to be routed to the outlet. A unit hydrograph is an empirical hydrologic method for representing a basin's
 125 outlet hydrograph from a known quantity of runoff uniformly available within a basin or zone for each modeled time step. This
 126 approach is available in the UNIT-HG model which computes a scaled time distribution of a unit depth of excess water over a
 127 given area from a rainfall-runoff model (National Weather Service 2005 and Linsley et al. 1982). Since SAC-SMA handles
 128 the timing of runoff through the soil column, the UNIT-HG model does not consider the excess water until it either becomes
 129 overland flow or enters the channel system (Anderson 2002). This routing method differs from traditional unit hydrograph
 130 approaches which consider interflow travel paths through the soil column as part of the unit hydrograph shape (Chow et al.
 131 1988). For basins with multiple zones, each zone has a separate UNIT-HG model and the zone hydrographs are added together to
 132 form the outlet hydrograph for the basin. We note that Unit Hydrographs and their parameters are not typically measurable,
 133 though in some cases they can be estimated from data in specific circumstances. See Section 4.8.2 for more details on how these
 134 parameters were estimated during calibration.

135 2.4 | Lag-K - Hydrologic Routing

136 Typically, the RFCs route a streamflow simulation downstream to the next forecast point using a hydrologic routing approach to
 137 capture lag and attenuation in the hydrograph. In lower river reaches where local inflow entering the stream channel between two
 138 forecast points is negligible, a hydrologic routing model is used exclusively. Conversely, when local inflow is significant, Lag-K
 139 is supplemented using additional SNOW-17, SAC-SMA, and UNIT-HG models. There are multiple hydrologic routing models

used by RFCs, but for this approach Lag-K was exclusively used. The lag parameter generates a shift in the hydrograph forward to represent travel time and the k parameter represents the attenuation of the streamflow as it travels downstream (Linsley et al. 1982). It is a flexible method of routing since both the lag and k elements can be either constant or a function of streamflow magnitude (National Weather Service 2002b). For this study, a lookup table was used for both the lag and k parameters based on upstream flow.

2.5 | Additional Models

There are three supplemental models utilized at the NWRFC. The use of these models for a particular basin depends on specific local conditions.

The CHANLOSS model accounts for losses or gains of water that occur along a channel reach as a result of interactions with groundwater, anthropogenic impacts, or evaporation from the stream surface (National Weather Service 2003a). The magnitude of these fluxes is calculated either as a percentage of the simulated streamflow or as a constant fixed value. Additionally, the model allows for temporal flexibility, enabling unique values to be defined for each month.

The CONS_USE model accounts for surface water diverted for irrigation based on crop ETD and irrigation efficiency (National Weather Service 2003b). It also includes a parameterized lagged return flow component, modeled similarly to SAC-SMA, using a single conceptual bucket. Other water demands, such as municipal and industrial use, can be captured using the CHANLOSS model.

Between the thirteen NWS RFCs, there are several different reservoir regulation models used: Single Reservoir Regulation Operations (RES-SNGL), Joint Reservoir Operations (RES-J), U.S. Army Corps of Engineers Hydrologic Engineering Center Reservoir System Simulation (HEC-ResSim), and SSARRESV. Generally, all these reservoir regulation models are used to model the effects of reservoir storage and releases on streamflows. NWRFC exclusively uses the SSARRESV model (National Weather Service 2004). The NWRFC coordinates with local water managers to input accurate regulations into these models operationally. Although used operationally, SSARRESV is not used in the model calibration process (see Section 3.2 for details).

3 | CALIBRATION DATA

3.1 | Meteorology Inputs

The NWS's Analysis of Record for Calibration (AORC) is a multi-decadal, high-resolution dataset containing all weather information necessary as forcings for land-surface and hydrologic models. It includes the period 1979-Present, hourly data on a 30'' (0.008333°) latitude/longitude grid. The primary motivation for developing this dataset was the need for a climatology-constrained near-surface weather record suitable for calibrating hydrologic models across the US (Fall et al. 2023).

The AORC variables used for this study are 2-meter above ground air temperature, specific humidity, terrain-level pressure, and precipitation accumulation. Variables other than precipitation are instantaneous at the start of the hour; precipitation accumulation ends at the given hour. We used specific humidity and terrain-level pressure grids to derive PTPS (Section 3.1.2). For each time step, basin or zone average air temperature, precipitation accumulation, and PTPS values were calculated and used as forcing input for the SNOW-17 model. The zone average air temperature was also used to calculate PET (Section 3.1.1).

3.1.1 | Dynamic Evapotranspiration

ETD is used as input to SAC-SMA and removes water from the model's soil tension water components. Monthly crop coefficient parameters PE_{adj} are used to convert the potential evaporation (PET) to ETD. Previous NWRFC operational SAC-SMA models used a static daily ETD regardless of basin conditions. For the new calibration approach, the Hargreaves-Samani equation was used to calculate daily PET (Hargreaves and Samani 1982). This equation is a temperature-indexed evaporation approach, but also incorporates extraterrestrial radiation (calculated based on latitude and day of year) given by

$$PET = C_1(T_a + 17.8)(R_e/\lambda)(T_x - T_n)^{C_2} \quad (1)$$

179 where T_a , T_x and T_n are daily average, max, and min temperatures, respectively, R_e is extraterrestrial radiation, λ is the latent
180 heat of vaporization, and C_1 and C_2 are fitting coefficients. Twelve unique calibrated C_1 coefficients were used, corresponding to
181 the 15th of each calendar month. For days in between the 15th, the coefficient was linearly interpolated using adjacent months.
182 As is common practice, C_2 was set to 0.5. Air temperature inputs were basin or zone averaged.

183 The PEadj parameters were derived using the remote sensing-based methodology established by Kamble et al. (2013). The
184 underlying remotely sensed dataset used was the Vegetation Index and Phenology Vegetation Indices due to its high temporal
185 overlap with the calibration period, gap-filled nature, and acceptable spatial resolution (5.6 km) (Didan et al. 2015 and Didan
186 and Barreto 2016). From the continuous data, basin or zone averaged monthly PEadj factors were calculated for the 15th of each
187 calendar month. Similarly to the C_1 coefficients, for days between the 15th of each month, the factors were linearly interpolated
188 using the adjacent months.

189 3.1.2 | Precipitation Typing

190 PTPS is one of the three inputs to the SNOW-17 model, and is used to partition the precipitation between rain or snow within the
191 model to aid in calculating RAIM and update internal model states (Figure 3, left). Historically, to derive PTPS the NWRFC
192 relied on a representative air temperature time series assigned to a specific basin elevation, lapse rate, and an area-elevation
193 curve. As part of this legacy process a static lapse rate was used, which would often be adequate over long temporal scales but
194 rarely was precise for individual storms.

195 For this recalibration effort, we used specific humidity and terrain-level pressure from the AORC gridded dataset to derive
196 surface wet-bulb temperatures. NWS Western Region guidance uses a standardized approach in which a wet-bulb temperature
197 of 0.5 °C is equivalent to the rain-snow level (Cleave et al. 2019). Based on this guidance, a terrain-level precipitation typing
198 grid was generated for each time step using a wet-bulb temperature threshold of 0.5 °C, where values below the threshold are
199 assigned a 1 (snow) and values above are assigned a 0 (rain). The binary grid values were converted into basin or zone averaged
200 time series of PTPS, which was used as input for the SNOW-17 model.

201 3.2 | Streamflow Data

202 Hydrologic models developed for operational forecasting by an RFC are typically set at locations that are also occupied by an
203 established measurement station that collects streamflow observations. Prior to beginning a calibration, we collected all subdaily
204 instantaneous and daily average streamflow observations at calibration sites for the same temporal period for which AORC data
205 were available (1979-present). When daily average streamflow was unavailable (e.g., the station was not established until after
206 the start of AORC availability), we imputed the daily average data.

207 Statistical estimation of missing streamflow records, also known as imputation, is a common practice for supplementing
208 hydrologic records with gaps in the observations. Traditional imputation methods include regression and resampling techniques
209 (Hirsch 1982 and Hamzah et al. 2021). Recently, machine learning approaches have been shown to be effective for imputing
210 hydrologic data (Wangwongchai et al. 2023). For this study, we imputed missing daily average streamflow data using the
211 MissForest algorithm (Stekhoven and Bühlmann 2011), a random forest-based algorithm implemented in the missRanger R
212 package (Mayer 2024). To assess the quality of the imputed data, we cross-validated the analysis using available streamflow
213 records by randomly dropping 50% of the data at a time and imputing the rest. We compared the imputed values to observations
214 and assessed performance using coefficient of determination (R^2), Nash-Sutcliffe Efficiency (NSE), and percent bias (PBIAS). We
215 repeated this analysis five times and averaged the results to assess overall imputation performance. Additionally, we performed
216 imputation using a linear regression model to provide a performance baseline. Performance of the MissForest algorithm is
217 generally very favorable with imputed values showing high R^2 and NSE and low bias. On average the MissForest imputation
218 algorithm performed 43% better than the linear regression model (average NSE of 0.90 vs. 0.58).

219 3.2.1 | Streamflow Data for Routing

220 Instantaneous and daily observed streamflow data were collected at upstream locations to serve as input for the Lag-K routing
221 model. Where data gaps existed in the daily record, values were imputed using the methodology discussed in Section 3.2.

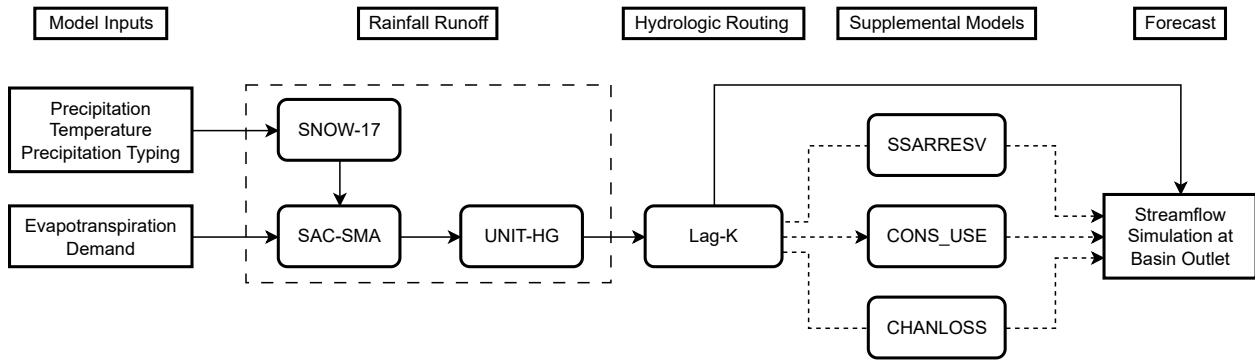


FIGURE 4 Flowchart of the NWRFC auto-calibration processes for utilization of the EDDS optimizer.

222 To produce a continuous subdaily time series, the CHPS AdjustQ methodology (Deltares 2021) was applied to merge
 223 instantaneous and daily observations. AdjustQ uses instantaneous data to "shape" the daily streamflow; for periods where
 224 instantaneous data are unavailable, simulated streamflow from the upstream model is used as a substitute.

225 The SSARRESV model was not recalibrated as part of this framework. Instead, when an upstream forecast point represented
 226 reservoir inflow, observed reservoir releases were used as the routing source. Similar to other locations, AdjustQ merged the
 227 instantaneous and daily release observations. However, for reservoir releases, no upstream simulation data were used to fill gaps
 228 in the instantaneous record; the merge relied strictly on the available observed datasets.

229 3.2.2 | Naturalized Streamflow Data

230 The NWRFC has an internally developed naturalized streamflow record at each of its forecast points with a period of record
 231 (POR) of 1980 to 2020. The dataset is used to establish climatological normals associated with its seasonal volume forecasts
 232 published by the NWRFC. For the dataset development, the effects of any upstream model use of CHANLOSS, CONS_USE, or
 233 SSARRESV to account for anthropogenic impacts are removed from the historical record. This dataset was used in this study to
 234 aid with the statistical clustering of modeled basins to establish parameter limits (Section 4.6) but not used directly for calibration.

235 4 | AUTOMATIC CALIBRATION

236 Auto-calibration of models attempts to estimate unknown parameters by comparing model output to observations and formulating
 237 an optimization problem to solve for the unknown parameters. The procedure involves selecting a calibration algorithm,
 238 identifying an appropriate objective function, choosing which parameters to optimize, and establishing their constraints (typically
 239 upper and lower limits). For each iteration, the optimizer selects a specific parameter set used to run the model, which is then
 240 compared against observations to compute the performance metric (objective function). The optimizer uses a specific algorithm
 241 to maximize the objective function value by modifying the unknown parameters within given limits. After a predetermined
 242 stopping criterion is reached (typically a pre-specified maximum number of iterations or a change tolerance between iterations),
 243 the optimizer stops and the final parameter set is further evaluated.

244 This section describes the methodology for auto-calibration used by the NWRFC for a single basin. The algorithm has
 245 interconnected processes, some of which continuously exchange information, in an effort to select NWRFC model parameters
 246 that best suit the selected objective function (Figure 4). Design decisions and special considerations associated with the processes,
 247 illustrated in Figure 4, are discussed in detail.

248 4.1 | Optimization Algorithm

249 A variant of the dynamically dimensioned search (DDS) algorithm (Tolson and Shoemaker 2007) was developed for optimization
 250 of model parameters. DDS has been recognized as a robust tool to perform hydrologic model optimizations (Arsenault et al.

251 2014). The DDS algorithm is not designed to find global optimal parameter values but instead to find reasonable parameter
252 values within a given computational budget (i.e. iteration limit). Initial NWRFC testing found that a 10,000-iteration DDS
253 run on a single CPU core yielded run times and performance comparable to other statistical optimizers. This was true even
254 when compared to algorithms like particle swarm optimization (PSO), which typically utilizes multiple cores and significantly
255 more iterations. The computational efficiency gained opened up the possibility that each CPU core could run an independent
256 auto-calibration of the DDS optimizer in parallel, with the best result from all of the parallel runs used as the final solution.
257 Running the DDS optimizer independently on multiple CPU cores simultaneously is referred to as an embarrassing parallel
258 approach (EP-DDS). Another parallel DDS implementation approach was explored by B.A. Tolson (2014) where, in contrast to
259 the EP-DDS approach, there are frequent routine check-ins to exchange information between the optimization runs on each CPU
260 core (P-DDS). Their study found that there is no clear winner between EP-DDS and P-DDS, but each has a distinct advantage
261 depending on how close an optimization run on each CPU core is to its iteration limit. B.A. Tolson (2014) stated that “The
262 next step in parallel DDS algorithm development involves merging the two parallel implementations to develop a parallel DDS
263 implementation that combines the best aspects of EP-DDS and P-DDS.”

264 Based on the strategies recommended by B.A. Tolson (2014) to utilize the strengths of both EP-DDS and P-DDS, we developed
265 a technique where the frequency of information exchange between independent parallel optimization processes increases as
266 iterations progress. For example with a 10,000 iteration budget, initially the parallel processes only exchange information every
267 1,000 iterations, to closely resemble a EP-DDS run. As the DDS run progresses, the frequency of check-ins increases from 1,000
268 to 500 to 100 to finally every 10 iterations. As the check in frequency increases, the DDS run more closely resembles the P-DDS
269 process. We call this method the evolving DDS (EDDS) algorithm. The approach resulted in improved run times compared to
270 EP-DDS and P-DDS, while still maintaining comparative calibration skill to other optimizers (Arsenault et al. 2014 and Asgari
271 et al. 2023). An auto-calibration run can be completed on a modern laptop in about 10 minutes.

272 4.2 | Objective Function

273 The NWRFC auto-calibration approach allows for the use of various objective functions. One simple choice for objective
274 function is to use one of the desired model performance metrics such as RMSE, NSE, Kling-Gupta Efficiency (KGE), and R^2 .
275 The objective function value can be calculated on either average daily flow data or instantaneous data at the model time step. In
276 practice, a single objective function often used with univariate optimization algorithms and multiple objectives are used with
277 specialized multi-objective optimization algorithms (Gupta et al. 1998). Alternatively, two or more objective functions can be
278 combined as a weighted sum and used as a univariate objective function values (Madsen 2000). This type of combined objective
279 function is a practical alternative to multiobjective optimization. While multiobjective approaches provide detailed information
280 about tradeoffs, they can be difficult to interpret in an operational setting where a single model solution is often preferable.

281 The choice of objective function is an important step in any calibration workflow and can significantly impact the calibrated
282 parameters and model performance. We explored different combinations of metrics and time steps to derive a suitable operational
283 model for site-specific needs. In general, we found that calibrations at the NWRFC are most successful when metrics are
284 combined to emphasize both location-specific high and low flows.

285 4.3 | Optimized Parameters

286 Calibrators configure the auto-calibration run by selecting models appropriate for the basin’s characteristics (e.g., local runoff,
287 routing, losses); however, the set of parameters optimized for those models is fixed. Generally, we did not optimize parameters if
288 we could observe or derive a measurable physical value for a specific basin. Examples of this would be basin area, mean elevation,
289 effective forest cover, travel time to the outlet, and latitude. Other parameters were not optimized when they represented the
290 limits of an assumed physical process. These were exclusively SNOW-17 parameters and they included: maximum negative
291 melt factor, antecedent snow temperature, base temperature for non-rain melt, maximum percent of liquid water held in the
292 snowpack, and daily melt at the snow-soil interface. In both instances, these parameters which are either measurable or represent
293 physical limits are referred to as static parameters. However, the majority of parameters associated with NWRFC models cannot
294 be directly linked to measurable basin attributes, and were optimized during the calibration process (Table 1).

295 For glacial zones, the SAC-SMA parameters *uztwm*, *lztwm*, *adimp*, *pctim*, *pfree*, and *riva*, as well as the SNOW-17 areal
296 depletion curve (ADC) and *si*, are not optimized. The SNOW-17 parameter *mbase* is only calibrated for glacial zones.

SNOW-17	SAC-SMA	Unit Hydrograph	Lag-K	CONS_USE	CHANLOSS
adc	adimp	shape	var_lag	accum_rate	adj_factor
mfmax	lzfpn	scale	var_K	decay_rate	
mfmin	lzfsn			irr_eff	
scf	lzpk				
si	lzsk				
uadj	lztwm				
mbase	pctim				
	pfree				
	rexp				
	riva				
	uzfwm				
	uzk				
	uztwm				
	zperc				

TABLE 1 Model parameters that are optimized as part of the auto-calibration procedure.

297 4.4 | Initial Conditions

298 Prior to executing any model run in the optimizer, reasonable initial model states must be established, which are commonly
 299 referred to as cold states. These states represent the pre-existing volume of water in the soil column, channel, or held frozen in
 300 the snowpack when the model is initialized. The start date of a model run is always set to October 1, so it can be assumed that
 301 there is no preexisting snowpack (with the exception of glacial zones). This assumption has been validated multiple times over
 302 the years by examining the SNOW-17 model states operationally and using regional snow observations. For glacial zones, the
 303 SNOW-17 snow depth is set to be large enough that it never fully melts, which represents year-round snow/ice cover. We also
 304 assume that for Lag-K states the upstream river reaches start the model run in baseflow conditions, which has been confirmed
 305 using streamflow observations.

306 Both SAC-SMA and CONS_USE models have components which represent the movement of water through the soil column
 307 using a series of linked conceptual buckets of known maximum capacity (uztwm, uzfwm, lztwm, lzfsn, and lzfpn in SAC-SMA
 308 and rfstor in CONS_USE). We use a spin-up technique to initialize the water content states at the onset of the auto-calibration
 309 run, following an approach similar to the North American Land Data Assimilation System (NLDAS) (Cosgrove et al. 2003).
 310 Using the parameters selected by the optimizer, the model is run iteratively for the first water year. At the end of each iteration
 311 (September 30), the final states are used to re-initialize the model at the start of the same water year (October 1), in the following
 312 iteration. This process repeats until the water content of each bucket at the beginning and end of the first water year converge
 313 (within a 1% tolerance) or a predefined iteration limit is reached. Once all the buckets have converged, those bucket volumes are
 314 adopted as the initial states. Although this is an empirical approach and not guaranteed to converge, it usually does, and tends to
 315 provide acceptable initial states for basins in the NWRFC domain under a wide range of hydrologic conditions. The first year of
 316 the simulation used for spin up is discarded when computing the objective function to account for any remaining transience in
 317 the initial states.

318 4.5 | Zone Delineation

319 Part of the NWRFC calibration process involves exploring if it is advantageous to split a basin into multiple discrete modeling
 320 zones. Breaking a basin into zones can be helpful for representing complex terrain, multiple land use types, or distinct dominant
 321 hydrologic processes which would not be well captured by a single lumped model. For each zone, meteorological forcings and
 322 static parameters are calculated prior to an auto-calibration run.

323 In the Western US, when snow is prevalent in a basin, two zones have often been used; one zone representing the higher
 324 elevations where snowpack persists through the winter and into the spring, and another zone where the snowpack is transient.
 325 During past calibrations, an elevation threshold was used to delineate the basin into upper and lower zones. For certain complex
 326 basins it is sometimes necessary to model the basin with more than two zones.

327 As part of the new calibration approach, we developed a method for zone delineation that incorporates several recent sources
 328 of hydrologic and land surface data (Table 2). The datasets were re-gridded to a common 1-km resolution and k-means clustering
 329 was used to classify basin grid cells into a pre-defined number of zones. Due to the role that orographic effects play in many of

330 the hydrologic characteristics utilized, the k-means clustering often followed elevation contours but with additional variability
 331 due to changes in forest cover, soil type, or basin aspect (Figure 5). A calibrator will extensively test and compare the appropriate
 332 number of zones for each model using performance metric associated with auto-calibration runs. We have found that two zones
 333 perform better at most locations with the exception of low elevation basins. Glacial regions, which are typically modeled as their
 334 own zone (see Section 2.1.1), were omitted from the k-means clustering.

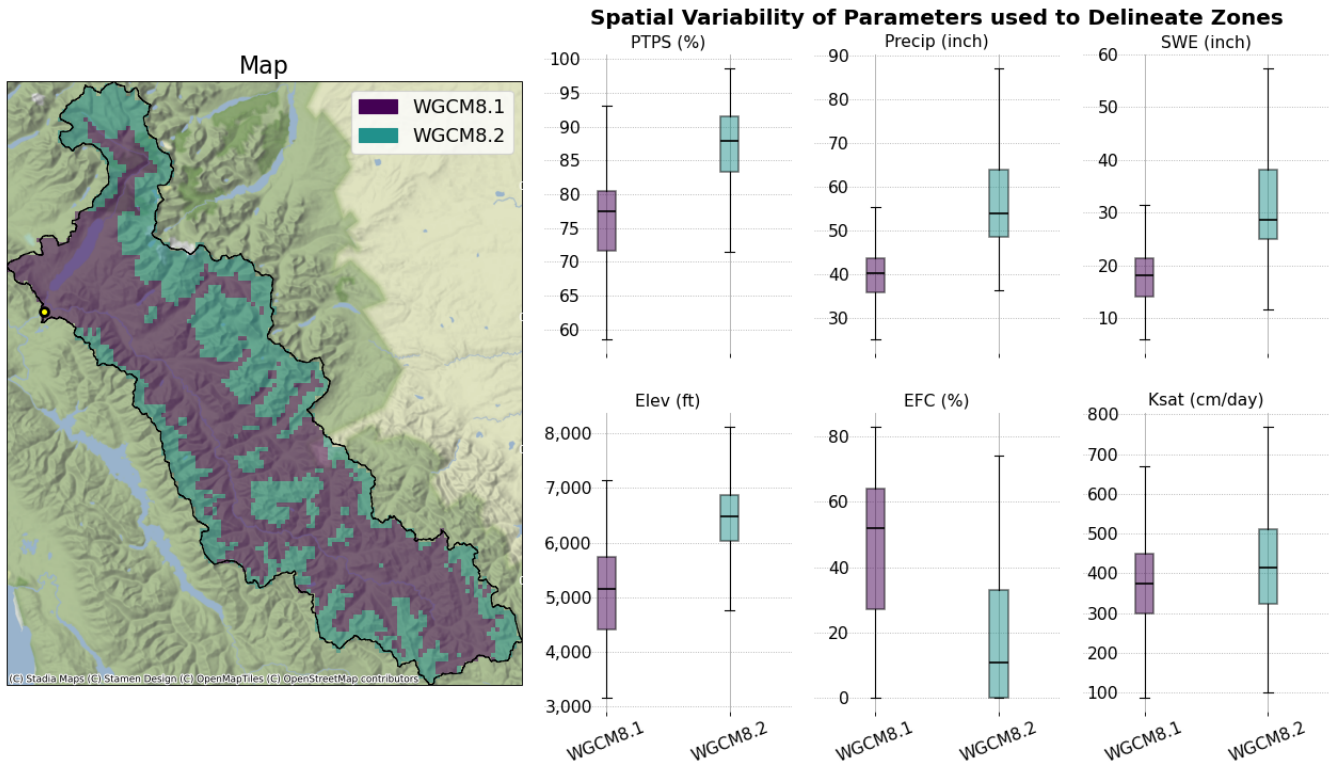


FIGURE 5 Example basin delineation using k-means clustering for the Middle Fork of the Flathead River near West Glacier, Montana. WGCM8.1 and WGCM8.2 indicate the two zones where zone 1 typically corresponds to lower elevations with the shortest travel time to the outlet. The yellow dot indicates the basin outlet.

Dataset	Data Source	Reference
Average PTPS from Nov-Mar	AORC	Fall et al. (2023)
Average Annual Precipitation Accumulation	AORC	Fall et al. (2023)
Topographical Elevation	USGS	U.S. Geological Survey (2023a)
Effective Forest Cover	NLCD, Canada	Beaudoin et al. (2014)
Saturated Hydraulic Soil Conductivity	Global Soil Hydraulic Properties	Zhang et al. (2018)
30day Avg Max Annual SWE depth	U Arizona	Zeng et al. (2018)
		Broxton et al. (2019)
30day Avg Max Annual SWE depth, Canada	ERA5-Land	Muñoz-Sabater et al. (2021)
		CCCS (2019)

TABLE 2 Hydrologic characteristics used for clustering and references for each dataset.

4.6 | Basin Parameter Limits

To define appropriate parameter limits for the optimizer, hierarchical clustering was performed to create groups from approximately 325 basins modeled by the NWRFC, ensuring that physically similar basins shared common constraints. Clustering was done using basin averaged hydrologic properties (Table 2) and average daily hydrograph shapes for each modeled basin. Initially, we clustered based on hydrologic properties alone, but the resulting groups were too hydroclimatically diverse. To address this diversity, we imposed a secondary constraint to ensure that groups also shared similar average naturalized hydrographs (Section 3.2.2). This was achieved by modifying the weights to the clustering features in an optimization algorithm which uses the correlation of the natural flow hydrographs of basins in a cluster to compute the objective function:

$$\max \sum_{k=1}^K q_{50}(C_k) \quad (2)$$

where K is the number of basin groups (clusters), $q_{50}(C_k)$ is a function that computes the median of all the elements of a matrix C_k , which is the correlation matrix of all the average natural flow hydrographs in a group of basins k .

This approach created groupings of basins which tended to be part of similar hydroclimatic regions (i.e. coastal, arid, etc.), which was adequate for the purposes of creating shared parameter limits. The number of clusters is somewhat arbitrary but should be determined based on the total number of basins to be modeled, the geographic diversity of the basins, and the desired number of groups. We used 25 clusters where each cluster had between 5 and 15 basins. See the supplemental material for details on each cluster of basins.

For each group of modeled NWRFC basins determined by the clustering algorithm, the optimizer parameter limits were collectively shared. This sharing of constraints is conceptually similar to the idea of hydrologic landscape regions (Leibowitz et al. 2016 and Patil et al. 2013). Parameter limits were informed by literature review, prior NWRFC calibration efforts for each basin in a group, NWSRFS calibration literature Anderson (2002), and trial and error. A final manual review of the limits in each cluster was conducted to ensure reasonable ranges were captured. See Appendix B for a list of typical parameter limits used in this study. We found that appropriate physically realistic parameter ranges are critical for mitigating equifinality (multiple parameter sets with similar objective function values) when using the NWSRFS suite of conceptual hydrologic models (Her et al. 2019).

In the absence of prior calibrations to help set parameter limits, we recommend using a combination of available literature and trial and error. One effective approach is to initially optimize a small subset of parameters while holding the others constant, then iteratively narrow the allowable ranges for that subset. This process can be repeated for other groups of parameters until distinct limits are established for the full set. Once reasonable bounds are determined, all parameters may be optimized simultaneously. Setting large ranges of all parameters simultaneously will likely lead to equifinality or optimizer convergence issues.

4.7 | Climatological Forcing Adjustments

Gridded meteorological observations datasets have some accepted level of spatial and temporal error at any particular grid cell because the data must be interpolated or estimated to derive a complete dataset (Lundquist et al. 2019). The AORC forcing dataset used for this study is no exception (Fall et al. 2023). Errors in gridded meteorological input data can lead to cumulative discrepancies in the model's water balance relative to observations, particularly during calibrations spanning multiple water years.

For the auto-calibration approach adopted by the NWRFC, we assumed that the errors in the AORC dataset relative to climatology could be multiplicative (scaling factors) or additive (bias) on a monthly scale. Adjustments were applied per basin and were allowed to vary independently for each forcing type (e.g. precipitation, air temperature, PTPS, and PET). The optimizer selected a single adjustment factor for each month, anchored to the 15th day of the month (Figure 6). This same value is applied to that month in every simulated year. To avoid abrupt steps between months, daily factors are linearly interpolated between these adjacent mid-month values. We converted the adjusted PET to ETD forcings for SAC-SMA using PEadj (Section 3.1.1).

The adjustment factors were subject to two key constraints. First, the resulting climatology for each forcing type in the calibration POR was required to stay within specific bounds defined by an external gridded dataset (Table 3). Second, to maintain temporal consistency, we imposed constraints using four parameters (Table 4) that preserve the relative ranking of monthly magnitudes, preventing unrealistic shifts in the seasonal cycle. Adjusting forcing data during hydrologic calibration is not standard practice. However, this approach is viable when the forcing data has known, complex biases relative to observations and a high-quality calibration is required. This adjustment technique is akin to an on-demand bias correction which is typically performed as a preprocessing step before calibration.

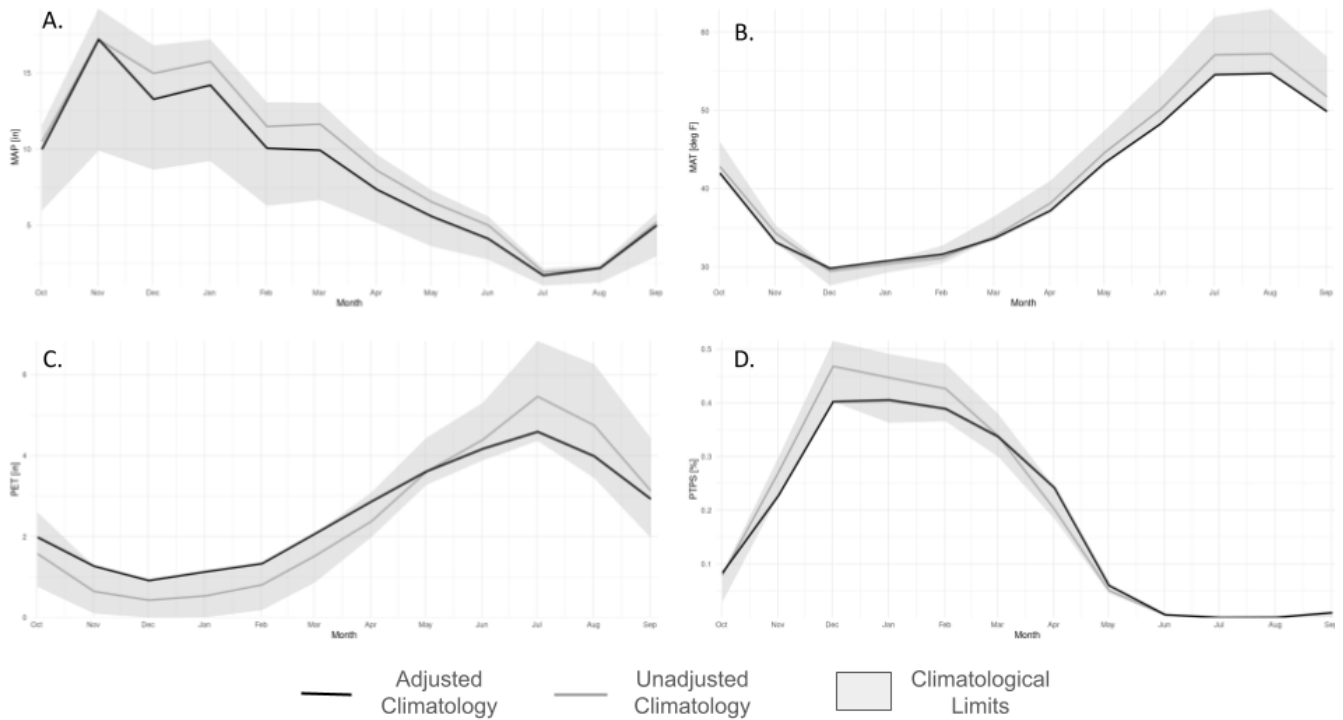


FIGURE 6 Examples of climatological monthly forcings before (grey line) and after adjustments (black line) applied through optimization during the auto-calibration routine. Imposed climatological limits used during optimization are also displayed (shaded area). A. precipitation (MAP), B. air temperature (MAT), C. evapotranspiration (PET), and D. precipitation typing (PTPS)

Precipitation Datasets	Reference
CHIRPS	(Funk et al. 2015)
ERA	Muñoz-Sabater et al. (2021)
NCAR	Newman et al. (2015)
PRISM	Daly et al. (2008)
Air Temperature Datasets	Reference
Daymet	Thornton et al. (2022)
ERA	Muñoz-Sabater et al. (2021)
NCAR	Newman et al. (2015)
TopoWX	Oyler et al. (2014)
Evapotranspiration Datasets	Reference
ERA	Muñoz-Sabater et al. (2021)
GLEAM	Miralles et al. (2011)
P-LSH	Zhang et al. (2015)
TerraClimate	Abatzoglou et al. (2018)
Precipitation Typing Datasets	Reference
ERA	Muñoz-Sabater et al. (2021)

TABLE 3 External gridded datasets for climatological forcing adjustment limits.

380 4.8 | Model Tables and Parameterized Curves

381 This section describes noteworthy design considerations for parameters that required more complex definition than simply
 382 selecting a single value within a range. These parameters represent tables or parameterized curves that require optimization
 383 while maintaining both physical realism and temporal consistency. The following subsections detail how these constraints were
 384 enforced by optimizing a small number of coefficients that parameterize the tables, rather than optimizing the entire table or
 385 curve. We also discuss how limits were imposed on these coefficients to maintain physically realistic processes.

Parameter	Description
f_mult	Multiplication factor to apply directly to the forcing.
p_redist	The percentage of the climatological forcing to redistribute.
std	Controls the weighting factor on how the p_redist is partitioned out to each climatological month based on ranking.
shift	Shift the climatological values by x numbers of days in the positive or negative direction.

TABLE 4 Climatological forcing adjustment parameters

4.8.1 | SNOW-17 - Derivation of Areal Depletion Curve

In order to apply SNOW-17 to an area, the model uses an ADC. The ADC is a relationship between the AESC and the basin's SWE Index. The SWE index is defined as the fraction of the current SWE relative to the season's maximum modeled SWE, which we refer to as the areal index (A_i). By design, both the AESC and the SWE index are normalized variables ranging from 0 to 1 and their relationship is expected to be physically reasonable and continuous. To ensure these two requirements are met, the following equation was used within the optimizer:

$$\frac{S}{A_i} = a \cdot A^b + (1 - a) \cdot A^c \quad (3)$$

where S is the SWE, A represents the AESC, and a , b , and c are parameters that were optimized with limits that ensured a physically reasonable result (see Appendix B). In practice, the ADC is typically discretized into 10 evenly spaced points.

As recommended by the Anderson calibration manual (Anderson 2002), the ADC was treated as a latent parameterization and no observed data was used to calibrate it directly. The three parameter curve shown in Equation 3 was developed to capture the full range of shapes of previous NWRFC ADCs. Including the ADC as a latent process contributes to the equifinality of the final parameter sets, but this allowed us to avoid the arbitrary manual process used in the past.

4.8.2 | UNIT-HG - Optimization of Unit Hydrograph

Each zone within a basin needs its own UNIT-HG model to route overland flow and channel runoff to the basin outlet. The model is based on a synthetic gamma distribution unit hydrograph (Croley 1980), which has associated shape and scale parameters that need to be calibrated. When using a single zone, the UNIT-HG parameters can be inferred from data using baseflow separation methods, but when using multiple zones for a basin the UNIT-HG parameters are latent and unobservable and so must be calibrated.

To constrain the shape of the unit hydrograph, we estimated the maximum travel time for overland flow and channel runoff using the method proposed by Maidment et al. (1996). First, we derived an overland flow velocity grid from USGS National Hydrologic Dataset (NHD) slope and flow accumulation data (U.S. Geological Survey 2023b), limiting velocities to a range of 0.02 to 2 m/s. By combining this velocity field with NHD flow direction grid, we calculated the maximum travel time to the basin outlet. This value served as a physical constraint during optimization, limiting the shape and scale parameters to those that produce a unit hydrograph duration (i.e., time base) within 25% of the calculated maximum travel time.

For prior NWRFC calibrations, duplicate unit hydrographs were used for each zone. With the inclusion of auto-calibration, each zone had its own optimized unit hydrograph using the calculated maximum travel time to the basin outlet. In practice, this flexibility improves calibrations by allowing the model to better capture the nuances of both rapid runoff and baseflow. However, in some cases, this added freedom exacerbates the equifinality of the solution space and causes something akin to label switching in hidden Markov models (Bracken et al. 2014 2016). For example, we observed instances where the hydrologic roles of the zones switched between successive optimization runs due to stochasticity in the optimizer. For example, a zone acting as the baseflow component in one run might switch to become the flashy component in a subsequent run. This issue was generally avoided by careful use of parameter limits or a reconsideration by the calibrator of the number of zones used to model the basin.

4.8.3 | Lag-K - Derivation of Variable Lag and K Tables

The Lag-K model characterizes upstream tributaries using two lookup tables for the lag and k parameters. As with the SNOW-17 ADC, these curves are constrained to be physically realistic and smooth. The specific values were determined using:

$$\text{lag or k table entry } i = d(Q_i - g)^2 + eQ_i + f \quad (4)$$

421 where d , e , f , and g were optimized and Q_i represents streamflow for the i th.

422 Upper and lower limits for the lag and K tables were established using historical streamflow observations at the upstream point
 423 and estimated travel times derived from an assumed velocity range of 1.6 to 11 km/h. Furthermore, restrictions were applied to
 424 the lag curve's parameter limits to guarantee a monotonic decrease in travel time as streamflow increases.

425 4.9 | Manual Calibration Review

426 At the NWRFC, when the calibrations are developed using the objective framework presented here, a final "human in the loop"
 427 step is conducted before a calibration is approved for operations. The overall objective of this process is to assess the quality of
 428 the parameterized model produced by the auto-calibration tool and to ensure it does not represent a degradation in performance
 429 compared to the current hydrologic model utilized operationally.

430 In this step an expert human forecaster reviews all the automatically calibrated parameters and examines the model output for
 431 inconsistencies or errors. Manual edits can be made to any of the optimized parameters by the calibrator to further improve
 432 performance. This step incorporates expert local knowledge and helps to mitigate the equifinality for which conceptual hydrologic
 433 models are especially prone (Her et al. 2019). If any issues are identified, they tend to indicate data issues or parameter limits
 434 that need to be refined before a new run of the auto-calibration is done.

435 5 | ACCOMPANYING SOFTWARE PACKAGES

436 As part of this calibration effort we sought to improve access to the original NWSRFS Fortran code and provide modern interfaces
 437 to the full suite of models used by the RFCs for operational forecasting (see Section 2). To this end, we created packages in
 438 R (rfchydromodels) and Python (py-rfchydromodels) that call the original NWSRFS Fortran 77 source code (via Fortran 90
 439 wrappers). The original code has undergone minimal updates to allow it to compile and run on modern systems and the code has
 440 been verified to be functionally equivalent to the Java-based implementation used in CHPS. The packages and documentation
 441 are available here: <https://github.com/NOAA-NWRFC/nwsrfs-hydro-models>. Community contributions are welcome.

442 6 | CALIBRATION RESULTS - CAMELS BASINS

443 The CAMELS dataset is a widely used benchmark dataset for calibration and comparative modeling studies (Newman et al.
 444 2015 2022). There are 38 CAMELS basins that share an outlet with an NWRFC forecast point. In this section we provide results
 445 for our calibrated models at these points.

446 Calibration studies often use a single objective function such as RMSE or NSE which is minimized to produce an optimal
 447 parameter set (Chouaib et al. 2021 and Arsenault et al. 2014 and Hogue et al. 2000). Both metrics rely on squared deviation
 448 between observed and simulated values, which put more weight on high flows. This unequal weighting can misrepresent low
 449 flows, which can be just as important as high flows to water managers in the Pacific Northwest due to their impacts to hydropower,
 450 fish management, navigation, and recreation. For these reasons we selected a combined objective function which balances low
 451 and high flows

$$\max \sum_i \text{NSE}(s_i - o_i) + \text{NSE}(\log(s_i) - \log(o_i)) \quad (5)$$

452 where s_i is the simulated flow, and o_i is the observed flow at time step i . Note that the model was run at a 6-hour time step but the
 453 objective function was computed for daily average values.

454 Figure 7 shows cumulative distribution functions (CDFs) of four commonly used metrics: NSE, PBIAS, R^2 , and KGE. All
 455 metrics besides R^2 have been normalized (nNSE, nKGE, nPBIAS; See Appendix A) to facilitate comparison on a common axis.
 456 The figure provides CDFs for calibrations of 27 basins in the NWRFC domain using three modeling approaches: (1) calibrations
 457 of the NWSRFS models using auto-calibrated framework described in this paper (black line), (2) calibrations of the NWSRFS
 458 models using the legacy NWRFC manual approach (orange line), and (3) a trained LSTM deep learning model from Kratzert

et al. (2024). Note that the LSTM was trained on 531 basins across contiguous US and we compute the ensemble mean from the 27 available CAMELS basins that are also NWRFC basins.

In overall quality the auto-calibrations and the legacy manual calibrations exhibit similar performance overall which is notable due to the large difference in the calibration times between the two methods (hours vs days). These auto-calibration metrics are shown prior to any human-in-the-loop adjustments which may improve the results further. The LSTM model tends to outperform calibrated conceptual models in terms of nNSE, which favors mean behavior and weights higher flows more strongly. However, nKGE performance is similar; the LSTM's larger bias offsets its higher R^2 values. These results indicate that for the NWRFC domain an auto-calibrated conceptual model can rival the quality of both expert manual calibrations and state-of-the-art deep learning models at a fraction of the human time and overall computational cost, respectively. We note that basins in the Pacific Northwest tend to perform relatively well in large sample hydrologic modeling studies and this level of quality may not be achievable in other regions (Newman et al. 2015).

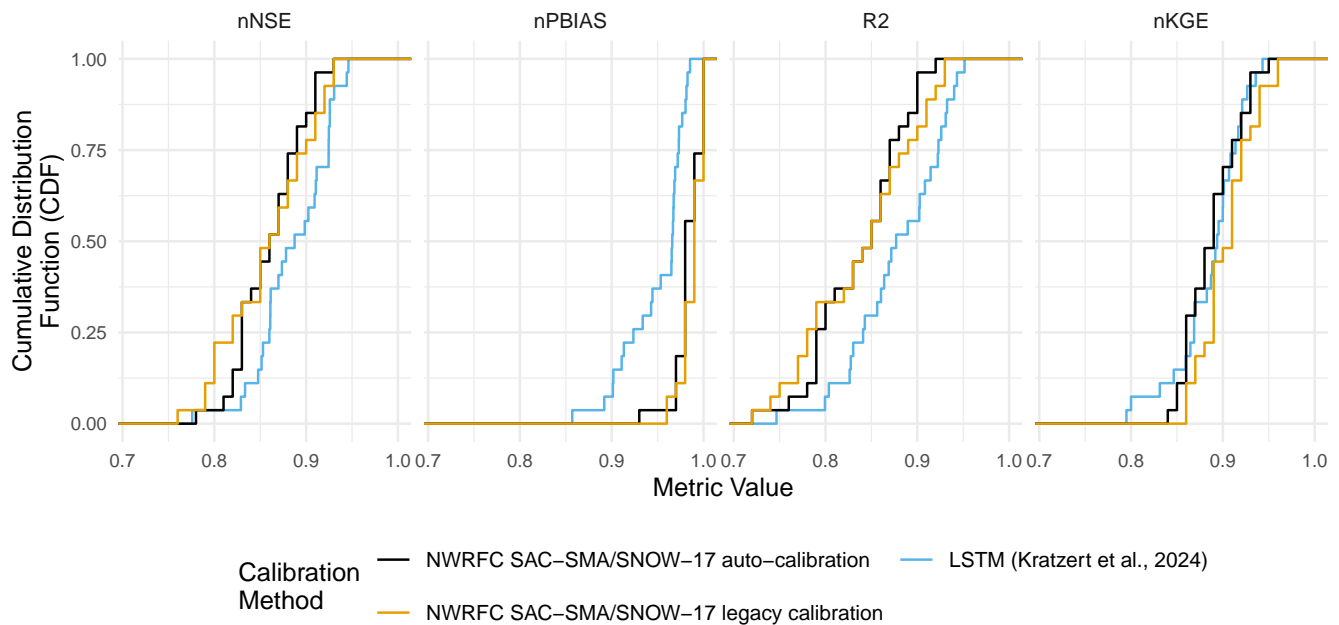


FIGURE 7 CDF of metrics scores from 27 basins in the NWRFC domain comparing NWRFC calibrations and metrics from a trained LSTM model from Kratzert et al. (2024). All basins are part of the CAMELS dataset. See Appendix A for definitions of the normalized metrics as well as tables of metrics for each basin.

The second set of results is shown in Figure 8, a Budyko diagram (Chen and Sivapalan 2020) for each of the 38 CAMELS basins that share a NWRFC forecast point. A Budyko diagram displays the limits (energy or water) of a basin based on long term averages of ET and precipitation which play a strong role in its overall hydrologic behavior. Basins in the NWRFC domain are typically energy limited due to ample precipitation but some basins particularly on the east side of the Cascade Range can be water limited. We used the KGE metric to evaluate the calibrations (Gupta et al. 1999). Any value above -0.41 indicates a calibration better than the mean, and values closer to 1 indicate better alignment with observations (Knoben et al. 2019). The high performance scores (KGE 0.75–0.98) observed across the domain illustrate that the calibration framework effectively captures the wide range of hydrologic conditions across the Budyko space.

7 | CALIBRATION RESULTS - CASE STUDIES

In this section we provide a detailed look at the calibration results of three representative CAMELS basins in the NWRFC domain (Figure 1). The first is the Nehalem R near Foss, Oregon (USGS #14301000, NWS ID FSSO3), which is a rain dominated

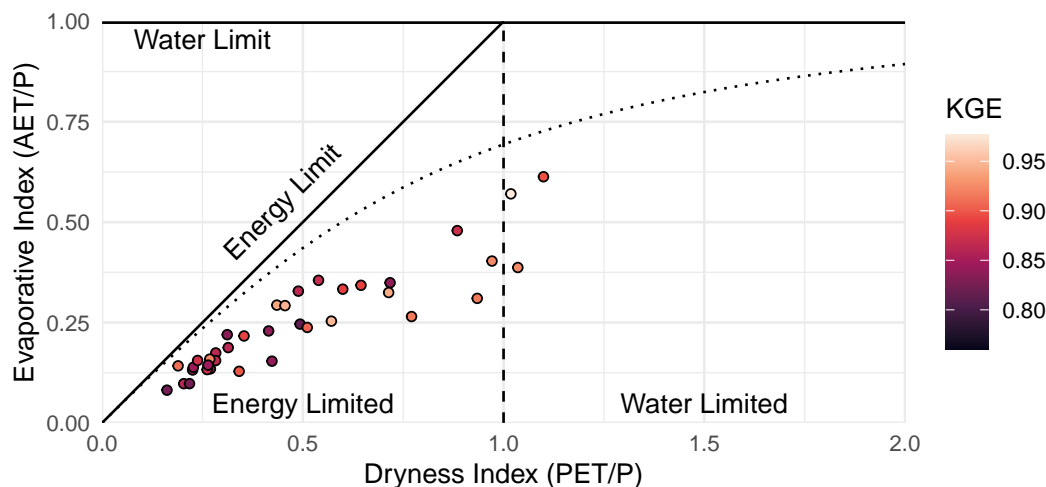


FIGURE 8 Budyko diagram showing long term behavior of the calibrated simulations for each zone of the three test basins. AET = Actual Evapotranspiration, P=Precipitation, PET=Potential Evapotranspiration, where all values represent long term annual averages, typically 10 years or more.

481 basin with a winter peak and limited snowmelt. The second is the Middle Fork of the Flathead River near West Glacier, Montana
 482 (USGS #12358500, NWS ID WGCM8), which is a snow melt dominated basin with a summer peak and limited winter rainfall.
 483 The third is the Sauk River Near Sauk, WA (USGS #12189500, NWS ID SAKW1), which is a basin with Lag-K routed upstream
 484 inflow and both winter rain and summer snowmelt.

485 To demonstrate the framework's flexibility in modeling diverse hydrologic conditions, Figure 9 compares continuous
 486 simulations with observed streamflow for the three CAMELS basins. These plots highlight the 2019–2022 period, a representative
 487 subset of the full POR calibration record (1980–2022). The POR parameters represent the calibration that is used operationally
 488 by the NWRFC. The modeled time series (orange) shows good agreement with observations (black), though divergences occur
 489 during peak flows and along some falling limbs. This divergence is likely due to the combined objective function which equally
 490 weights low and high flows at a daily time step. Figure 10 shows cyclical plots which combine the entire POR continuous
 491 simulation. Each year of simulation (1980–2022) is overlaid on the same Julian day and the 10th and 90th percentiles are
 492 computed for each day, which is represented by the gray bands. The median of the POR simulations is shown in blue and the
 493 median of the observed data is shown in black. Cyclical plots can quickly pinpoint structural errors in hydrologic models. It is
 494 desirable to see the median of the observations fall within the simulation band and ideally close to observed median, which is the
 495 case for each of these basins.

496 It is common modeling practice to split the available data record into an independent calibration and a validation period to
 497 ensure the calibrated parameters are robust and reliable when the model is used in periods outside of the training data. Models
 498 which have notable differences in performance between the calibration and validation periods may suffer from overfitting.
 499 Overfitting is a situation in which a model fits well to observed data used for calibration but performs poorly when used on
 500 unobserved conditions. While it is typically not a large concern in physically based modeling, it is a concern here due to the
 501 flexibility of the conceptual NWSRFS models and the numerous latent parameters optimized by the auto-calibration approach.
 502 To ensure the auto-calibration results are robust and reliable (i.e. not overfit), we used two validation techniques to test for
 503 this issue: cross-validation (CV) and stationary bootstrapping (SB). We used 4 CV periods, also known as “folds” denoted
 504 CV1 through CV4, using 3/4 of the total data as a calibration period and the remaining period (approximately 10 years) as an
 505 independent validation period for each fold. There was no temporal overlap between the 1/4 of the data used for validation
 506 from each fold. SB is a resampling technique to aid in identifying optimization parameter overfitting (Politis and Romano 1994
 507 and Politis and White 2004 and Patton et al. 2009). The approach works by randomly sampling complete water years from
 508 the POR simulation and stitching them together until it has an equivalent length to the CV fold's validation period. For each
 509 randomly sampled record, model performance metrics were computed. In total 24,000 SB records, of approximately 10 years,
 510 were sampled for each of the three basins. For a model that is not overfit, the CV metrics should fall within the distribution of the

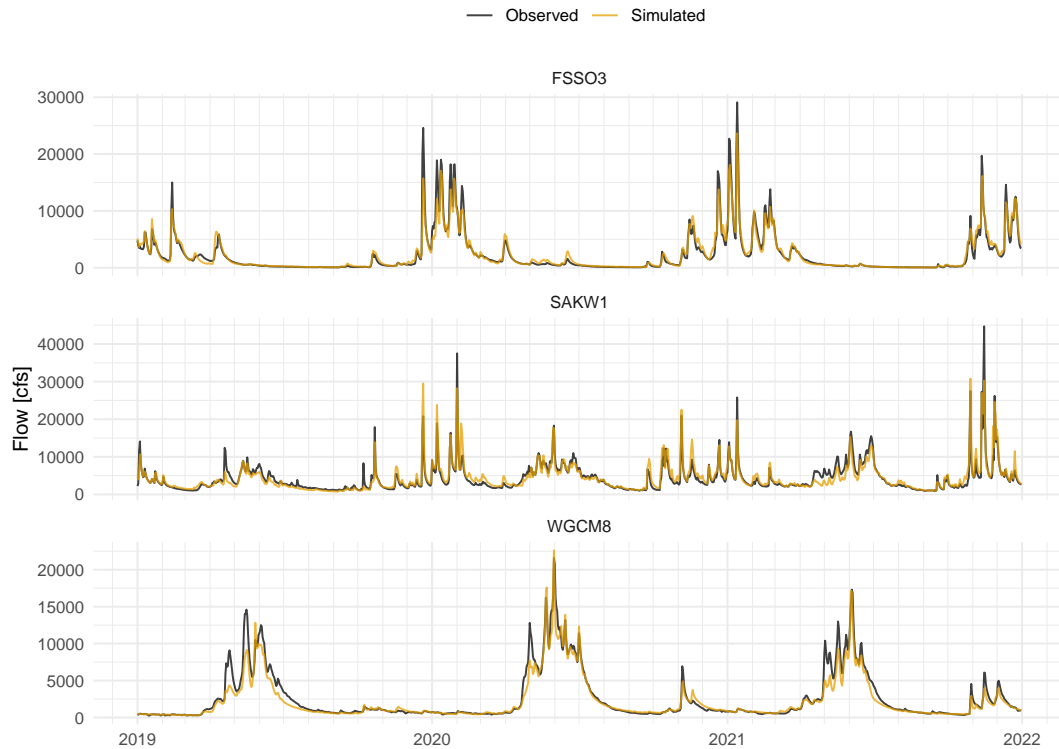


FIGURE 9 Calibrated continuous simulations (2019–2022) for three diverse CAMELS basins within the NWRFC domain. The black line represents the observed streamflow, while the blue line represents the simulated streamflow.

511 resampled SB metrics. Figure 11 shows the nNSE, nPBIAS, R^2 , and nKGE metric scores for each CV fold validation period
 512 and compares them to the distributions generated by the SB method, which is presented as a violin plot. The stability of metric
 513 scores across the CV folds and their alignment with the SB runs in Figure 11 indicates that the auto-calibration found similarly
 514 optimal solutions and that the resulting parameter sets are not overfit to the calibration data.

515 The NWRFC utilized a climatological forcing adjustment technique (Section 4.7) to allow for corrections of forcing inputs
 516 during optimization. To demonstrate both the value added by the technique and that the additional model flexibility does not
 517 suffer from overfitting, Figure 11 compares results with climatological forcing adjustments and those without. For all three basins
 518 the addition of the climatological forcing adjustments does not result in overfitting, as the CV fold scores in comparison to the
 519 SB results are similar whether the method is or is not used. At SAKW1 and WGCM8, the forcing adjustment run provides minor
 520 improvement across all metrics, but at FSSO3 the forcing adjustments dramatically improve the validation results, indicating a
 521 potential issue with the raw AORC forcings in this basin. These results also indicate that including forcing corrections may not
 522 benefit every basin but they do not degrade the performance when used.

523 8 | DISCUSSION AND CONCLUSIONS

524 In this paper, we present a comprehensive framework developed by the NWRFC for calibration of hydrologic basins in the
 525 Pacific Northwest US. The framework includes snow, soil moisture, routing, channel loss, and consumptive use models. Data
 526 inputs include a wide range of open-access sources for meteorological inputs, observed streamflow, land use, topography, and
 527 land cover. The framework can account for basins with diverse hydrologic conditions, from rain-dominated to snowmelt-driven.
 528 We have also developed a flexible, objective auto-calibration system that can handle numerous unmeasurable or latent model
 529 parameters in a computationally efficient manner. A full auto-calibration run can typically be completed on a modern laptop in
 530 under 10 minutes. In addition, we have made accompanying R and Python packages available for the entire suite of NWSRFS

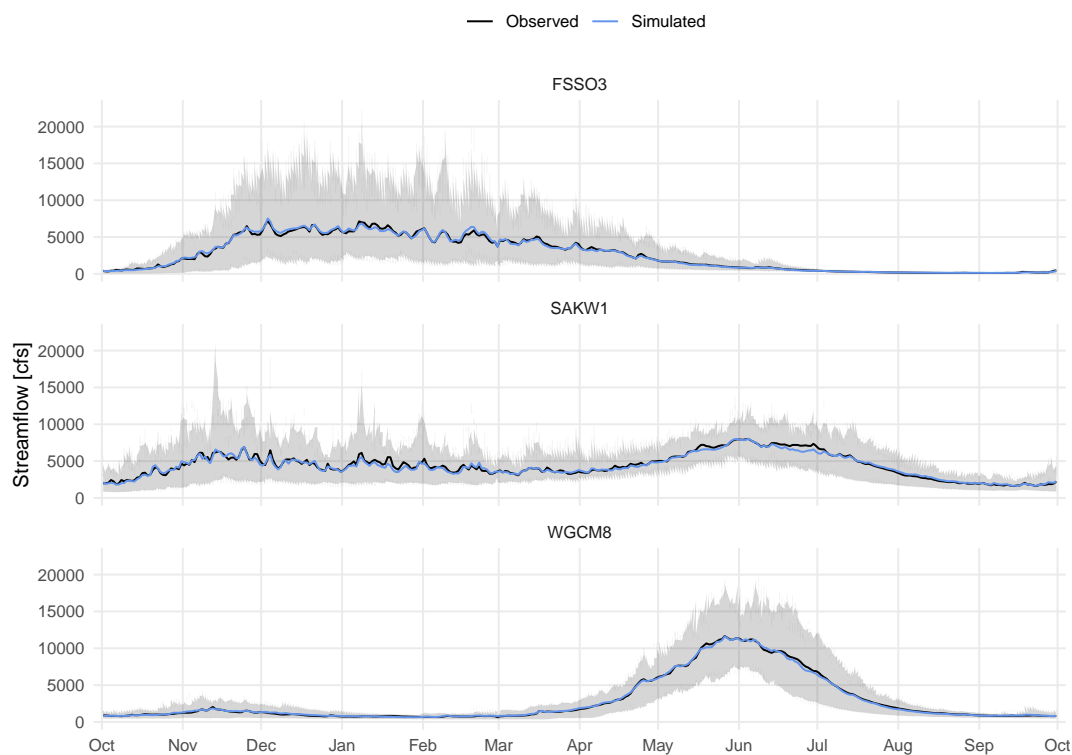


FIGURE 10 Cyclical streamflow plots showing the daily hydrologic regime from 1980 to 2022. The black line represents the median observed streamflow, while the blue line represents the median simulated streamflow. The grey shaded area indicates the 10th to 90th percentile range of the simulations.

531 models, including SAC-SMA, SNOW-17, and Lag-K. These modern interfaces are intended to increase the accessibility of these
532 models and facilitate future research.

533 We presented results where we applied this calibration approach at CAMELS basins that are also NWRFC forecast locations,
534 which are representative of the broader set of basins calibrated by the NWRFC. The calibration framework performed well
535 overall, with KGE values ranging from 0.75 to 0.96. From this broader set, we presented detailed results for three specific basins
536 selected for their distinct runoff characteristics (rain, snowmelt, and mixed rain/snowmelt). We provided simulation results
537 from the POR run in comparison to the observed streamflow by presenting a sample of the result from Water 2019 through
538 2022 and cyclical plot from the full POR calibration record (Figures 9 and 10). In both plots, the simulation is capturing the
539 streamflow response from both winter rainfall and spring snowmelt. The CV results combined with SB have been shared for the
540 three CAMELS basins which provide evidence that the auto-calibration is successfully avoiding the pitfall of model overfitting
541 (Figure 11). The CV and SB results compare performance with and without the climatological forcing adjustment. The findings
542 demonstrate that the approach mitigates aleatory uncertainty in meteorological inputs without inducing overfitting or degrading
543 model performance.

544 In Figure 7, we present results for 27 CAMELS basins which illustrate that the parameterizations produced by the auto-
545 calibration framework are on par with the performance of legacy NWRFC manually calibrated NWSRFS models. It is not
546 surprising that manual calibrations conducted by expert hydrologists perform better in some basins, however the auto-calibration
547 results shared were produced at a fraction of the human cost and time. In the past, manual calibrations took up to a week of
548 dedicated time from an expert calibrator for each basin whereas now multiple basins can be calibrated in the same amount of time.

549 In recent years, the rising use of artificial intelligence and machine learning (AIML) models in hydrology has called into
550 question whether traditional hydrologic modeling approaches still have utility (Nearing et al. 2021). We have demonstrated that
551 in the Pacific Northwest US, calibrated lumped conceptual models can rival the performance of a state of the art LSTM deep
552 learning model (Figure 7) at a fraction of the computational cost. The results presented in this paper can serve as a benchmark
553 for new and emerging AIML approaches. In the future we would like to perform calibrations at all CAMELS basins and present

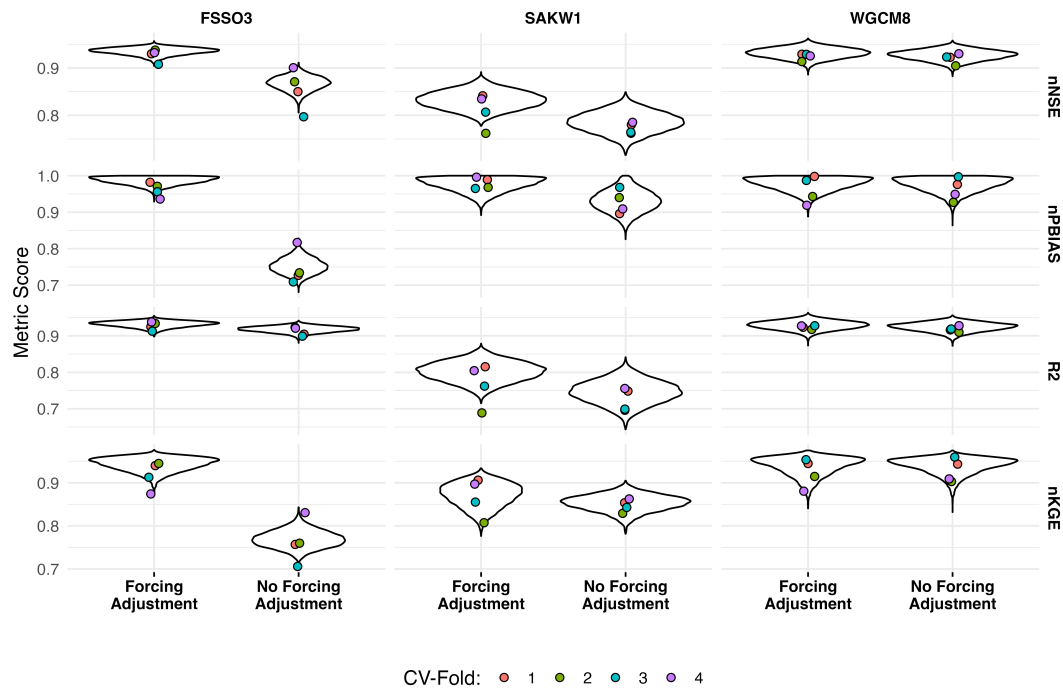


FIGURE 11 Cross validation (points) and POR bootstrapping (violin plots) metric scores with and without using climatological forcing adjustments

554 the results for benchmarking. An interesting extension of this would involve additional detailed comparisons between new AIML
 555 models and the calibrations used in our framework in an attempt to identify where both might be combined or further improved.

556 One limitation of this framework is that it cannot represent tidally-influenced basins. Such basins require a nonlinear hydraulic
 557 model to solve for the tidal influence at the outlet. These hydraulic models are significantly more computationally expensive to
 558 run than the conceptual model and was therefore prohibitive to auto-calibrate. Another limitation is that the auto-calibration
 559 process does not include reservoir regulation. Regulation is a critical piece of operational hydrologic forecasting. In practice this
 560 is done through specialized regulation models or real-time coordination with reservoir operators.

561 We consider this framework and the calibrations it produces to set a new standard for what is possible with lumped conceptual
 562 models. This approach reduces the overall resources required when compared to both manual calibrations (labor hours) and AIML
 563 model training (computational cost), and enables rapid re-calibrations as new data becomes available. We have demonstrated
 564 here that with careful data curation of an objective calibration framework, combined with expert local knowledge, can produce
 565 high quality lumped conceptual hydrologic model calibrations that can be used successfully in operational hydrologic forecasting.
 566 The NWRFC currently uses this approach to calibrate basins which in turn are being used to produce operational flood warnings
 567 and seasonal water volume forecasts.

568 DATA AND CODE

569 All data used in this paper for analysis and figure generation, including the auto-calibration output is available here: <https://zenodo.org/records/18408868>. The code used to generate the figures in this paper is here: <https://github.com/NOAA-NWRFC/JAWRA-calibration-paper-figs>. The wrapper packages for SAC-SMA, SNOW-17 and the remaining NWSRFS models is here: <https://github.com/NOAA-NWRFC/nwsrfs-hydro-models>. The automatic calibration code is available here: <https://github.com/NOAA-NWRFC/nwsrfs-hydro-autocalibration>.

574 AUTHOR CONTRIBUTIONS

575 Geoffrey Walters – Conceptualization, Data Curation, Formal Analysis, Investigation, Methodology, Project Administration,
 576 Software, Validation, Visualization, Writing – Original Draft Preparation, Writing – Review & Editing; Cameron Bracken –
 577 Conceptualization, Data Curation, Formal Analysis, Investigation, Methodology, Software, Validation, Visualization, Writing
 578 – Original Draft Preparation, Writing – Review & Editing; Brad Gillies – Conceptualization, Formal Analysis, Investigation,
 579 Writing – Review & Editing; Leah Pope – Formal analysis, investigation, Methodology, Writing – Review & Editing; Henry Pai

580 – Conceptualization, Formal Analysis, Investigation, Writing – Review & Editing; Sonali Chokshi – Investigation, Writing –
581 Review & Editing; Victor Stegmiller – Investigation, Writing – Review & Editing; Julie Bracken - Formal Analysis, Writing
582 – Review & Editing; Stephen King – Supervision, Writing – Review & Editing; Taylor Dixon – Project Administration,
583 Supervision, Resources, Writing – Review & Editing; Joe Intermill – Supervision, Writing – Review & Editing.

584 ACKNOWLEDGMENTS

585 Many thanks to all the NWRFC staff (past and present) including Amy Burke, Evan Simpson, Catherine Fitzpatrick, Bruce
586 Anderson, Ryan Lucas, and Phil Butcher.

587 CONFLICT OF INTEREST

588 The authors declare no potential conflict of interests.

589 REFERENCES

- 590 Abatzoglou, John T., et al. “TerraClimate, a High-Resolution Global Dataset of Monthly Climate and Climatic Water Balance from 1958–2015.”
591 *Scientific Data*, vol. 5, no. 1 January 2018).
- 592 Anderson, Eric. *Calibration of Conceptual Hydrologic Models for Use in River Forecasting*, 2002.
- 593 Arsenaault, Richard, et al. “Comparison of Stochastic Optimization Algorithms in Hydrological Model Calibration.” *Journal of Hydrologic Engineering*,
594 vol. 19, no. 7 July 2014), pp. 1374–1384.
- 595 Asgari, Marjan, et al. “Development of a Knowledge-Sharing Parallel Computing Approach for Calibrating Distributed Watershed Hydrologic Models.”
596 *Environmental Modelling & Software*, vol. 164 June 2023), pp. 105708.
- 597 B.A. Tolson, D.A. Swayne, V. Sharma. “Parallel Implementations of the Dynamically Dimensioned Search (DDS) Algorithm.” *Environmental Software*
598 *Systems*, vol. 573, 2014.
- 599 Beaudoin, A., et al. “Mapping Attributes of Canada’s Forests at Moderate Resolution through kNN and MODIS Imagery.” *Canadian Journal of Forest*
600 *Research*, vol. 44, no. 5 May 2014), pp. 521–532.
- 601 Bracken, C., et al. “Spatial Bayesian Hierarchical Modeling of Precipitation Extremes over a Large Domain.” *Water Resources Research*, vol. 52, no. 8,
602 2016, pp. 6643–6655.
- 603 Bracken, C., et al. “A Hidden Markov Model Combined with Climate Indices for Multidecadal Streamflow Simulation.” *Water Resources Research*,
604 vol. 50, no. 10, 2014, pp. 7836–7846.
- 605 Broxton, Patrick, et al. “Daily 4 Km Gridded SWE and Snow Depth from Assimilated In-Situ and Modeled Data over the Conterminous US, Version
606 1.” 2019.
- 607 Burnash, Robert J. C., et al. *A Generalized Streamflow Simulation System : Conceptual Modeling for Digital Computers*. , National Weather Service,
608 1973.
- 609 CCCS. “ERA5-Land Hourly Data from 1950 to Present.” 2019.
- 610 Chen, Xi, and Murugesu Sivapalan. “Hydrological Basis of the Budyko Curve: Data-guided Exploration of the Mediating Role of Soil Moisture.”
611 *Water Resources Research*, vol. 56, no. 10 October 2020).
- 612 Chouaib, Wafa, et al. “Implications of a Priori Parameters on Calibration in Conditions of Varying Terrain Characteristics: Case Study of the SAC-SMA
613 Model in Eastern United States.” *Hydrology*, vol. 8, no. 2 May 2021), pp. 78.
- 614 Chow, Ven Te, et al. *Applied Hydrology*, McGraw Hill, 1988.
- 615 Cleave, Darren Van, et al. *Snow Level in the NWS Western Region: Definition and Calculation Methodology*. , National Weather Service, 2019.
- 616 Cosgrove, Brian, et al. “NOAA’s National Water Model: Advancing Operational Hydrology through Continental-Scale Modeling.” *JAWRA Journal of*
617 *the American Water Resources Association*, vol. 60, no. 2, 2024, pp. 247–272.
- 618 Cosgrove, Brian A., et al. “Real-Time and Retrospective Forcing in the North American Land Data Assimilation System (NLDAS) Project.” *Journal of*
619 *Geophysical Research: Atmospheres*, vol. 108, no. D22, 2003.
- 620 Croley, Thomas E. “Gamma Synthetic Hydrographs.” *Journal of Hydrology*, vol. 47, no. 1–2 May 1980), pp. 41–52.
- 621 Daly, Christopher, et al. “Physiographically Sensitive Mapping of Climatological Temperature and Precipitation across the Conterminous United
622 States.” *International Journal of Climatology*, vol. 28, no. 15 March 2008), pp. 2031–2064.
- 623 Deltares. “AdjustQ - DELFT-FEWS Documentation.” 2021. Accessed: May 2021.
- 624 Didan, K, and A Barreto. “NASA MEaSURES Vegetation Index and Phenology (VIP) Vegetation Indices 15 Days Global 0.05 Deg CMG [Data Set].
625 NASA EOSDIS Land Processes DAAC 4.” 2016.
- 626 Didan, K, et al. “Multi-Sensor Vegetation Index and Phenology Earth Science Data Records: Algorithm Theoretical Basis Document and User Guide.”
627 *Vegetation Index and Phenology Lab, University of Arizona: Tucson, AZ, USA*, , 2015.
- 628 Fall, Greg, et al. “The Office of Water Prediction’s Analysis of Record for Calibration, Version 1.1: Dataset Description and Precipitation Evaluation.”
629 *JAWRA Journal of the American Water Resources Association*, vol. 59, no. 6 July 2023), pp. 1246–1272.
- 630 Feng, Dapeng, et al. “Differentiable, Learnable, Regionalized Process-Based Models With Multiphysical Outputs Can Approach State-Of-The-Art
631 Hydrologic Prediction Accuracy.” *Water Resources Research*, vol. 58, no. 10, 2022, pp. e2022WR032404.
- 632 Funk, Chris, et al. “The Climate Hazards Infrared Precipitation with Stations—a New Environmental Record for Monitoring Extremes.” *Scientific*
633 *Data*, vol. 2, no. 1 December 2015).
- 634 Gupta, Hoshin Vijai, et al. “Toward Improved Calibration of Hydrologic Models: Multiple and Noncommensurable Measures of Information.” *Water*
635 *Resources Research*, vol. 34, no. 4 April 1998), pp. 751–763.
- 636 Gupta, Hoshin Vijai, et al. “Status of Automatic Calibration for Hydrologic Models: Comparison with Multilevel Expert Calibration.” *Journal of*
637 *Hydrologic Engineering*, vol. 4, no. 2 April 1999), pp. 135–143.
- 638 Hamzah, Fatimah Bibi, et al. “A Comparison of Multiple Imputation Methods for Recovering Missing Data in Hydrological Studies.” *Civil Engineering*
639 *Journal*, vol. 7, no. 9 September 2021), pp. 1608–1619.

- 640 Hargreaves, George H., and Zohrab A. Samani. "Estimating Potential Evapotranspiration." *Journal of the Irrigation and Drainage Division*, vol. 108,
641 no. 3 September 1982), pp. 225–230.
- 642 Her, Younggu, et al. "Uncertainty in Hydrological Analysis of Climate Change: Multi-Parameter vs. Multi-GCM Ensemble Predictions." *Scientific*
643 *Reports*, vol. 9, no. 1 March 2019).
- 644 Hirsch, Robert M. "A comparison of four streamflow record extension techniques." *Water Resources Research*, vol. 18, no. 4 July 1982).
- 645 Hogue, Terri S., et al. "A Multistep Automatic Calibration Scheme for River Forecasting Models." *Journal of Hydrometeorology*, vol. 1, no. 6
646 December 2000), pp. 524–542.
- 647 Kamble, Baburao, et al. "Estimating Crop Coefficients Using Remote Sensing-Based Vegetation Index." *Remote Sensing*, vol. 5, no. 4 March 2013),
648 pp. 1588–1602.
- 649 Knoben, Wouter J. M., et al. "Technical Note: Inherent Benchmark or Not? Comparing Nash–Sutcliffe and Kling–Gupta Efficiency Scores." *Hydrology*
650 *and Earth System Sciences*, vol. 23, no. 10 October 2019), pp. 4323–4331.
- 651 Konapala, Goutam, et al. "Machine Learning Assisted Hybrid Models Can Improve Streamflow Simulation in Diverse Catchments across the
652 Conterminous US." *Environmental Research Letters*, vol. 15, no. 10 September 2020), pp. 104022.
- 653 Kratzert, Frederik, et al. "HESS Opinions: Never Train a Long Short-Term Memory (LSTM) Network on a Single Basin." *Hydrology and Earth*
654 *System Sciences*, vol. 28, no. 17 September 2024), pp. 4187–4201.
- 655 Kratzert, Frederik, et al. "Towards Learning Universal, Regional, and Local Hydrological Behaviors via Machine Learning Applied to Large-Sample
656 Datasets." *Hydrology and Earth System Sciences*, vol. 23, no. 12 December 2019), pp. 5089–5110.
- 657 Leibowitz, Scott G., et al. "Hydrologic Landscape Characterization for the Pacific Northwest, USA." *JAWRA Journal of the American Water Resources*
658 *Association*, vol. 52, no. 2 February 2016), pp. 473–493.
- 659 Linsley, R.K., et al. *Hydrology for Engineers*, McGraw-Hill Series in Water Resources and Environmental Engineering. McGraw-Hill, 1982.
- 660 Lundquist, Jessica, et al. "Our Skill in Modeling Mountain Rain and Snow Is Bypassing the Skill of Our Observational Networks." *Bulletin of the*
661 *American Meteorological Society*, vol. 100, no. 12 December 2019), pp. 2473–2490.
- 662 Madsen, H. "Automatic Calibration of a Conceptual Rainfall–Runoff Model Using Multiple Objectives." *Journal of Hydrology*, vol. 235, no. 3 August
663 2000), pp. 276–288.
- 664 Maidment, D. R., et al. "Unit Hydrograph Derived from a Spatially Distributed Velocity Field." *Hydrological Processes*, vol. 10, no. 6, 1996, pp.
665 831–844.
- 666 Mayer, Michael. *missRanger: Fast Imputation of Missing Values*, 2024.
- 667 Miralles, D. G., et al. "Global Land-Surface Evaporation Estimated from Satellite-Based Observations." *Hydrology and Earth System Sciences*, vol. 15,
668 no. 2 February 2011), pp. 453–469.
- 669 Muñoz-Sabater, Joaquín, et al. "ERA5-Land: A State-of-the-Art Global Reanalysis Dataset for Land Applications." *Earth System Science Data*, vol.
670 13, no. 9 September 2021), pp. 4349–4383.
- 671 Nash, J. E., and J. V. Sutcliffe. "River Flow Forecasting through Conceptual Models Part I — A Discussion of Principles." *Journal of Hydrology*, vol.
672 10, no. 3 April 1970), pp. 282–290.
- 673 National Weather Service. *National Weather Service River Forecast System User Manual: Conceptualization of the Sacramento Soil Moisture*
674 *Accounting Model*. National Oceanic and Atmospheric Administration, 2002. Release 81, Part II, Chapter II.3.
- 675 National Weather Service. *National Weather Service River Forecast System User Manual: Lag and K Routing*. National Oceanic and Atmospheric
676 Administration, 2002. Release 81, Part II, Chapter II.4.
- 677 National Weather Service. *National Weather Service River Forecast System User Manual: Channel Loss Operations*. National Oceanic and Atmospheric
678 Administration, 2003. Release 81, Part V, Chapter V.3.3.
- 679 National Weather Service. *National Weather Service River Forecast System User Manual: Consumptive Use Operations*. National Oceanic and
680 Atmospheric Administration, 2003. Release 81, Part II, Chapter II.4.
- 681 National Weather Service. *National Weather Service River Forecast System User Manual: SSARR Reservoir Regulation Operation*. National Oceanic
682 and Atmospheric Administration, 2004. Release 81, Part II, Chapter II.4.
- 683 National Weather Service. *National Weather Service River Forecast System User Manual: Unit Hydrograph*. National Oceanic and Atmospheric
684 Administration, 2005. Release 81, Part II, Chapter II.4.
- 685 National Weather Service. *National Weather Service River Forecast System User Manual: Snow Accumulation and Ablation Model - SNOW-17*.
686 National Oceanic and Atmospheric Administration, 2006. Release 81, Part I, Chapter II.2.
- 687 Nearing, Grey S., et al. "What Role Does Hydrological Science Play in the Age of Machine Learning?." *Water Resources Research*, vol. 57, no. 3,
688 2021, pp. e2020WR028091.
- 689 Newman, A. J., et al. "Development of a Large-Sample Watershed-Scale Hydrometeorological Data Set for the Contiguous USA: Data Set
690 Characteristics and Assessment of Regional Variability in Hydrologic Model Performance." *Hydrology and Earth System Sciences*, vol. 19, no. 1
691 January 2015), pp. 209–223.
- 692 Newman, Andrew J., et al. "Gridded Ensemble Precipitation and Temperature Estimates for the Contiguous United States." *Journal of Hydrometeorology*,
693 vol. 16, no. 6 November 2015), pp. 2481–2500.
- 694 Newman, Andrew J., et al. "CAMELS: Catchment Attributes and MEteorology for Large-sample Studies." June 2022.
- 695 Oyler, Jared W., et al. "Creating a Topoclimatic Daily Air Temperature Dataset for the Conterminous United States Using Homogenized Station Data
696 and Remotely Sensed Land Skin Temperature: TOPOCLIMATIC DAILY AIR TEMPERATURE." *International Journal of Climatology*, vol. 35, no.
697 9 August 2014), pp. 2258–2279.
- 698 Patil, Sopan D., et al. "Use of Hydrologic Landscape Classification to Diagnose Streamflow Predictability in Oregon." *JAWRA Journal of the American*
699 *Water Resources Association*, vol. 50, no. 3 November 2013), pp. 762–776.
- 700 Patton, Andrew, et al. "Correction to "Automatic Block-Length Selection for the Dependent Bootstrap" by D. Politis and H. White." *Econometric*
701 *Reviews*, vol. 28, no. 4 January 2009), pp. 372–375.
- 702 Politis, Dimitris N., and Joseph P. Romano. "The Stationary Bootstrap." *Journal of the American Statistical Association*, vol. 89, no. 428 December
703 1994), pp. 1303–1313.
- 704 Politis, Dimitris N., and Halbert White. "Automatic Block-Length Selection for the Dependent Bootstrap." *Econometric Reviews*, vol. 23, no. 1
705 December 2004), pp. 53–70.
- 706 Schaake, J., et al. "The Hydrologic Ensemble Prediction Experiment (HEPEX).", October 2006).

- 707 Shen, C. “Deep Learning: A Next-Generation Big-Data Approach for Hydrology.” *Eos* April 2018.
- 708 Stekhoven, Daniel J., and Peter Bühlmann. “MissForest—Non-Parametric Missing Value Imputation for Mixed-Type Data.” *Bioinformatics (Oxford,*
- 709 *England)*, vol. 28, no. 1 October 2011), pp. 112–118.
- 710 Thornton, M.M., et al. “Daymet: Monthly Climate Summaries on a 1-Km Grid for North America, Version 4 R1.”, 2022.
- 711 Tolson, Bryan A., and Christine A. Shoemaker. “Dynamically Dimensioned Search Algorithm for Computationally Efficient Watershed Model
- 712 Calibration.” *Water Resources Research*, vol. 43, no. 1 January 2007).
- 713 U.S. Geological Survey. “1/3rd Arc-Second Digital Elevation Models (Dems) - USGS National Map 3DEP Downloadable Data Collection.” 2023.
- 714 U.S. Geological Survey. “National Hydrography Dataset Plus High Resolution (NHDPlus HR).” 2023. Accessed: 2024-02-04.
- 715 Wangwongchai, Angkool, et al. “Imputation of Missing Daily Rainfall Data; A Comparison between Artificial Intelligence and Statistical Techniques.”
- 716 *MethodsX*, vol. 11 October 2023), pp. 102459.
- 717 Zeng, Xubin, et al. “Snowpack Change from 1982 to 2016 over Conterminous United States.” *Geophysical Research Letters*, vol. 45, no. 23 December
- 718 2018).
- 719 Zhang, Ke, et al. “Vegetation Greening and Climate Change Promote Multidecadal Rises of Global Land Evapotranspiration.” *Scientific Reports*, vol.
- 720 5, no. 1 October 2015).
- 721 Zhang, Yonggen, et al. “A High-resolution Global Map of Soil Hydraulic Properties Produced by a Hierarchical Parameterization of a Physically
- 722 Based Water Retention Model.” *Water Resources Research*, vol. 54, no. 12 December 2018), pp. 9774–9790.

723 □

724 APPENDIX

725 A NORMALIZED MODEL PERFORMANCE METRICS

726 Definitions of Nash-Sutcliffe Efficiency (NSE) Nash and Sutcliffe (1970), Kling-Gupta Efficiency (KGE) (Gupta et al. 1998),

727 and percent bias (PBIAS) are widely reproduced in the literature so we will not include them here, but the normalized versions

728 of these metrics are not as widely known. Normalization primarily helps with visualization because the metrics fall in a fixed

729 range of [0, 1]. The interpretation of these metrics is slightly different but analogous to the non-normalized versions. Table A1

730 provides the normalization formulas, viable ranges, and reference values for each metric.

Metric	Normalization Formula	Original Range	Normalized Range	Model Mean Reference	Perfect Score
nNSE	$\frac{1}{2 - \text{NSE}}$	$(-\infty, 1]$	$[0, 1]$	0.5	1
nPBIAS	$1 - \frac{ \text{PBIAS} }{100}$	$(-\infty, \infty)$	$(-\infty, 1]$	varies	1
R^2	None	$[0, 1]$	—	0	1
nKGE	$\frac{1}{2 - \text{KGE}}$	$(-\infty, 1]$	$[0, 1]$	0.415	1

TABLE A1 Performance metrics and their normalized versions. For NSE, a value of 0 indicates model performance equal to using the observed mean as the prediction (nNSE = 0.5). For KGE, a value of -0.41 indicates performance equal to the mean (nKGE = 0.415). PBIAS measures bias as a percentage, where 0 indicates no bias. The coefficient of determination (R^2) is already bounded between 0 and 1, where 0 represents no correlation (equivalent to predicting the mean).

731 B AVERAGE PARAMETER LIMITS FOR THE OPTIMIZER FOR ALL CAMELS BASINS IN THE NWRFC

732 DOMAIN

	param name	lower	upper	mean
1	adc_a	0.00	0.25	0.25
2	adc_b	0.05	50.00	49.95
3	adc_c	0.50	50.00	49.50
4	adimp	0.00	0.20	0.20
5	lzfpm	146.99	546.62	399.63
6	lzfsm	45.38	156.71	111.34
7	lzpk	0.00	0.01	0.01
8	lzsk	0.06	0.19	0.14
9	lztwm	69.47	235.40	165.93
10	mfmax	0.62	1.17	0.55
11	mfmin	0.13	0.38	0.25
12	pctim	0.00	0.05	0.05
13	pfree	0.14	0.53	0.38
14	rexp	1.30	3.42	2.12
15	riva	0.00	0.20	0.20
16	scf	0.70	1.50	0.80
17	si	1.00	5000.00	4999.00
18	uadj	0.06	0.17	0.11
19	unit_shape	1.01	3.30	2.29
20	unit_toc_adj	0.75	1.25	0.50
21	uzfwm	28.67	87.64	58.97
22	uzk	0.20	0.47	0.27
23	uztwm	41.70	112.19	70.49
24	zperc	24.00	156.66	132.66

TABLE B2 Average lower and upper parameter limits as well as the average actual optimized value for all 38 CAMELS basins in the NWRFC region.